



## Abstract

There is an increasing number of DEMs available worldwide for deriving elevation differences over time, including vertical changes on glaciers. Most of these DEMs are heavily post-processed or merged, so that physical error modelling becomes impossible and statistical error modelling is required instead. We propose a three-step methodological framework for assessing and correcting DEMs to quantify glacier elevation changes: remove DEM shifts, check for elevation-dependent biases, and check for higher-order, sensor-specific biases. An analytic, simple and robust method to co-register elevation data is presented in regions where stable terrain is either plentiful (case study New Zealand) or limited (case study Svalbard). The method is exemplified using the three global elevation data sets available, SRTM, ICESat and the ASTER GDEM, and with automatically generated DEMs from satellite stereo instruments of ASTER and SPOT5-HRS. After three-dimensional co-registration, significant biases related to elevation were found in some of the stereoscopic DEMs. Biases related to the satellite acquisition geometry (along/cross track) were detected at two frequencies in the automatically generated ASTER DEMs. The higher frequency bias seems to be related to satellite *jitter*, most effective in the back-looking pass of the satellite. The origins of the more significant lower frequency bias is uncertain. ICESat-derived elevations are found to be the most consistent globally available elevation data set available so far. Before performing regional-scale glacier elevation change studies or mosaicking DEMs from multiple individual tiles (e.g. ASTER GDEM), we recommend to co-register all elevation data to ICESat as a global vertical reference system. The proposed methodological framework is exemplified for elevation changes on the Fox, Franz Joseph, Tasman and Murchison glaciers of New Zealand and the glaciers of central Spitsbergen, Svalbard.

## Correcting elevation data for glacier change detection

C. Nuth and A. Kääb

Title Page

Abstract

Introduction

Conclusions

References

Tables

Figures



Back

Close

Full Screen / Esc

Printer-friendly Version

Interactive Discussion



# 1 Introduction

Applications of regional and global scale elevation products have increased substantially in geoscience. Surface elevation data are collected by many sensors using various techniques, and differencing between the multi-temporal elevation products is becoming a common method for monitoring surface changes, particularly of glaciers. The data are typically available as a continuous profile or swath of points, a network of points or a regular grid, the latter we will refer to as a Digital Elevation Model (DEM). There are three (nearly) global elevation products available to the public today. The Shuttle Radar Topography Mission (SRTM) in February 2000 provided the first product using interferometric SAR (InSAR) techniques (Farr et al., 2007). The ICESat mission from 2003 to 2009 provided the second using space-borne Light Detection and Ranging (Lidar) (Zwally et al., 2002). The third is the newly released ASTER GDEM based upon a composition of automatically generated DEMs from Advanced Spaceborne Emission and Reflection radiometer (ASTER) stereo scenes acquired from 2000–present (METI/NASA/USGS, 2009). Many of these products contain errors and biases resulting from sensor instabilities, limitations of the techniques, bad surveying conditions on the ground and various types of post-processing artifacts. The errors occur at a range of scales that directly affect measurement precision and increases the significance level an elevation change requires for adequate detection through elevation differencing.

The motivation behind this study is to address the accuracy of comparisons between the globally available elevation data sets with particular attention towards detecting glacier elevation changes. This involves classifying and understanding the errors and especially biases associated with each of the data products and to suggest corrections that may improve the accuracy and precision of the differences. Many of the data sets available to researchers today and those tested in this study are the result of second-level processing. This means that the conversion procedures between the original data acquisition (i.e. laser return waveforms, radar interferograms or stereo-imagery) to

TCD

4, 2013–2077, 2010

## Correcting elevation data for glacier change detection

C. Nuth and A. Kääb

Title Page

Abstract

Introduction

Conclusions

References

Tables

Figures

◀

▶

◀

▶

Back

Close

Full Screen / Esc

Printer-friendly Version

Interactive Discussion



final elevation data is lost and thus errors can not be anymore physically determined or modeled based upon the original transformation equations and acquisition parameters. Therefore, we use statistical approaches to analyze errors and to determine potential bias corrections. Even if physical modelling of errors might be preferable, an advantage of the statistical error modelling approach is that universal methods can be developed that may be widely applicable to different types of elevation data and irrespective of the sensor systems and processing procedures applied.

Detection of glacier elevation changes through DEM or elevation differencing is not a new procedure. Repeat photogrammetry was being used as early as in the 1950s to quantify the retreat of glaciers (Finsterwalder, 1954). Today, comparisons of elevation data acquired from space are becoming more popular in research because of the high temporal and spatial availability in remote areas where glaciers are present. Some studies use the data sets as they are, without searching or correcting for biases between them (e.g. Rignot et al., 2003; Sund et al., 2009; Muskett et al., 2009) which may lead to biased estimates of glacier volume changes or false-detection of surging (Berthier, 2010). The consequences of un-corrected biases in the previously named and other studies is not known to us. However, many studies search for biases between the data pairs and apply corrections using various methods (e.g. Berthier et al., 2007, 2010; Racoviteanu et al., 2007; Peduzzi et al., 2010).

The most important correction is to co-register the two elevation data products such that the pixels of each DEM represent the same spots on the Earth surface. Some studies co-register by minimizing the Root Mean Square Error (RMSE) of stable terrain elevation differences using a 2-dimensional linear regression, or in other words shifting one DEM to the other, for example within  $\pm 5$  pixels (Rodriguez et al., 2006; Berthier et al., 2007; Howat et al., 2008). Other studies have corrected DEMs using single or multiple linear regression corrections between elevation and the location and terrain parameters (Gorokhovich and Voustianiouk, 2006; Bolch et al., 2008; Peduzzi et al., 2010). In particular in terrestrial and airborne laser scanning, 3-dimensional least squares matching (LSM) is used to minimize the Euclidean distances between

## Correcting elevation data for glacier change detection

C. Nuth and A. Kääb

Title Page

Abstract

Introduction

Conclusions

References

Tables

Figures



Back

Close

Full Screen / Esc

Printer-friendly Version

Interactive Discussion



the points of point clouds, often allowing not only for shifts but also for rotations and scales between the two or more datasets (Gruen and Akca, 2005).

Another commonly applied correction to DEMs is an elevation dependent bias (Berthier et al., 2004, 2007, 2010; Kääb, 2008) which may arise due to an uneven distribution of ground control points (GCPs) or to inaccurate satellite parameters. This correction may have significant implications for glacier elevation changes because glaciers spread a range of altitudes which define their ablation and accumulation areas. At this point it should be noted that such elevation biases might result solely from differences in the resolution of the DEMs compared (Paul, 2008). Last, biases associated with the satellite acquisition geometry have been found in some products related to satellite attitude parameters which was shown to be significant enough to warrant a correction (Berthier et al., 2007). This type of correction will only apply to those data products where it is significant; e.g. satellite stereoscopic DEMs.

## 2 Objectives and case study locations

The objectives of this study is to present a simple and effective *universal* method to co-register elevation products. We aim at a method that can easily be applied without specialized software necessary and with a high degree of automation. We argue that this method should be used as a first step in elevation comparison due to the varying location accuracies of the different sensors. In a second step, after centering the two data products to each other, analysis of remaining anomalies is compiled to detect both linear and non-linear biases and to determine which errors require correction and how they affect glacier elevation changes. In contrast to the first step, the universal 3-dimensional co-registration, the procedures applied in the second and third steps are highly dependent on the sensor type and post-processing used for the elevation data. We will therefore only show examples for this secondary adjustments, using ASTER satellite stereo as a scenario.

### Correcting elevation data for glacier change detection

C. Nuth and A. Kääb

Title Page

Abstract

Introduction

Conclusions

References

Tables

Figures



Back

Close

Full Screen / Esc

Printer-friendly Version

Interactive Discussion



Two sites are chosen for this study. The first is the mid-latitude high alpine region of the southern Alps in New Zealand. The region is chosen because of its alpine glacier characteristics, high elevation range, and availability of stable terrain from which to exemplify the biases and derive corrections. In this case-study, SRTM, ICESat, ASTER GDEM, and automatically generated ASTER DEMs from the US Geological Survey Land Processes Distributed Active Archive Center (LPDAAC) are compared. The second site is the high Arctic alpine region of Svalbard where ground control is limited to nunataks and along the strandflats. Automatically generated DEMs from ASTER and SPOT5-HRS are used in combination with ICESat and an aero-photogrammetrically derived DEM.

### 3 Data

#### 3.1 Stereoscopic DEMs

Stereoscopic DEMs are generated using photogrammetric techniques from either ground-, air- or space- borne platforms. Measuring surface heights through photogrammetry relies on the principle of *parallax* which is “the apparent shift in the position of an object due to a shift in the position of the observer” (Mikhail et al., 2001). A parallax measurement gives the difference between the projected stereo rays of the same object onto the Earths ellipsoid and can be converted to height if the two observer positions and the focal length of the camera are known (Lillesand et al., 2004). The Base-To-Height (B/H) ratio is an apriori estimate of parallax precision based upon the stereo geometry (Toutin, 2008).

Air-borne stereo geometry is typically defined by overlapping vertical frame photography acquired under airplanes. Space-borne stereo geometry is constructed using either cross-track or along-track stereo constellations. The latter constellations consist of nadir and backward looking sensors (e.g. ASTER), forward and backward looking sensors (e.g. SPOT-5 HRS), forward, nadir and backward looking sensors (e.g. ALOS

## Correcting elevation data for glacier change detection

C. Nuth and A. Kääb

Title Page

Abstract

Introduction

Conclusions

References

Tables

Figures



Back

Close

Full Screen / Esc

Printer-friendly Version

Interactive Discussion



PRISM), or sensors that can be freely rotated to any stereo geometry (e.g. Ikonos, WoldView, Pleiades). Satellite stereoscopy is slightly more complicated than traditional photogrammetry as it uses pushbroom instead of frame sensors and must solve for additional unknown parameters related to the Earth's rotation and curvature (Toutin, 2004; Käab, 2005). Exterior image orientation can be computed from ground control points (GCP) and a satellite orbital model (Toutin, 2004) that is implemented in commonly available software like PCI Geomatica<sup>®</sup>. Automated approaches are becoming more common for deriving the relative and/or absolute orientation of stereo images using direct measurements of the satellite's attitude and position (i.e. pointing information, auxiliary and ancillary data) (for more details, see Schenk, 1999). The latter is the approach for both satellite stereo DEMs used in the this study: the ASTER DEMs produced by LPDAAC using the SilcAst software (product AST14) (Fujisada et al., 2005) and the SPOT5-HRS DEMs (Bouillon et al., 2006; Korona et al., 2009), as for instance available through the IPY SPOT SPIRIT program.

The stereoscopic ASTER instrument, in orbit since 1999 aboard the Terra platform, contains a nadir and backward VNIR sensor (0.76–0.86  $\mu\text{m}$ ) separated by  $\approx 30^\circ$  corresponding to a B/H ratio of 0.6 (ERSDAC, 2005; Toutin, 2008). The ground swath is 60 km while the image and DEM ground resolution is 15 and 30 m, respectively. The HRS instrument, aboard the SPOT5 satellite since 2002, contains forward and backward panchromatic sensors (0.48–0.7  $\mu\text{m}$ ), both  $20^\circ$  from nadir providing a B/H ratio of 0.8 (Berthier and Toutin, 2008). The 120 km ground swath is twice as large as ASTER, with a ground pixel resolution of 10 m across track and 5 m along track, and a final DEM resolution of 40 m (Korona et al., 2009).

Errors associated with stereoscopic DEMs are related to the errors in the orientations of the stereo-scenes, either from GCP-based solutions or direct on-board determination, and to the ability of the matching algorithms to locate the corresponding points on two or more images. Errors in the parallax determination are both due to imperfect matching procedures and due to the imperfect image quality such as from lack of optical contrast, cloud cover, shadows, topographic distortions, etc. Errors related to the

## Correcting elevation data for glacier change detection

C. Nuth and A. Käab

[Title Page](#)[Abstract](#)[Introduction](#)[Conclusions](#)[References](#)[Tables](#)[Figures](#)[Back](#)[Close](#)[Full Screen / Esc](#)[Printer-friendly Version](#)[Interactive Discussion](#)

parallax matching often result in blunders rather than bias, whereas errors related to the image orientation will typically induce bias. ASTER DEM accuracy is reported to be typically within 15–60 m RMSE in the vertical depending upon terrain type (Toutin, 2002, 2008; Kääb et al., 2002; Hirano et al., 2003; Kääb, 2005; Fujisada et al., 2005) and between 15 and 50 m horizontally (Fujisada et al., 2005; Iwasaki and Fujisada, 2005). SPOT5 accuracy is reported to be between 10–25 m vertically (Berthier and Toutin, 2008; Korona et al., 2009) and greater than 15 m in the horizontal (Bouillon et al., 2006; Berthier and Toutin, 2008). In relationship to pushbroom sensors (e.g. ASTER and SPOT5 HRS), it has been shown that variation in the satellites attitude induces biases within the raw images acquired as well as final DEMs produced (Leprince et al., 2007; Berthier et al., 2007).

### 3.2 Interferometric DEMs

The Shuttle Radar Topography Mission (SRTM), launched in February 2002, mapped the Earth from 60° N to 56° S using single-pass synthetic aperture radar (SAR) interferometry (Farr et al., 2007). SAR interferometry uses the phase differences between two radar images acquired using a small base-to-height ratio. These phase differences are the photogrammetric equivalent to a “parallax” measurement allowing retrieval of topography (Rosen et al., 2000). We use the SRTM3, V2 without void filling (NASA et al., 2002). Many glacier elevation change studies have used this as a base dataset to compare to both newer and older data products (Rignot et al., 2003; Berthier et al., 2004; Larsen et al., 2007; Schiefer et al., 2007; Paul and Haeberli, 2008). Typically reported vertical accuracies of the dataset are  $\approx \pm 10$  m which is lower than the mission standards of  $\pm 16$  m (Rodriguez et al., 2006). However, vertical biases are present due to instability of the sensor and/or platform (Rabus et al., 2003), and elevation-dependent biases have also been shown due to penetration of the C-band Radar waves into snow/ice (Rignot et al., 2001; Berthier et al., 2004, 2006).

## Correcting elevation data for glacier change detection

C. Nuth and A. Kääb

Title Page

Abstract

Introduction

Conclusions

References

Tables

Figures



Back

Close

Full Screen / Esc

Printer-friendly Version

Interactive Discussion



### 3.3 Lidar profiles

In 2003, the NASA Ice, Cloud, and land Elevation Satellite (ICESat) was launched with the Geoscience Laser Altimeter System (GLAS) acquiring elevation measurements in a 40–70 m elliptical footprint every 170 m (Zwally et al., 2002). The rapid failure of the first laser invoked a curtailed orbital acquisition program. Nonetheless, the GLAS lasers operated for the following 5 years before the last laser failed in November 2009. The altimeter has proven to be accurate to within  $\pm 15$  cm over flat deserts (Fricker et al., 2005), and intersection accuracies over low sloped glaciers on the order of  $\pm 1$  m (Brenner et al., 2007; Moholdt et al., 2010a), although variations between the GLA06 and GLA14 products may vary up to  $\pm 3$  m. ICESat products are freely available from NSIDC ([www.nsidc.org](http://www.nsidc.org)), and are the third global elevation product publicly available and tested in this study. ICESat has been extremely successful for glacier applications in terms of elevation changes (Howat et al., 2008; Pritchard et al., 2009; Moholdt et al., 2010b) but also for determining the accuracy of newer satellite products (Korona et al., 2009) and older topographic maps (Nuth et al., 2010). ICESat release 531 is used for this study; the GLA14 products (Zwally et al., 2010b) are used for analysis of stable terrain whereas analysis of ice is using the GLA06 product (Zwally et al., 2010a). Mean elevation differences between these products have been previously found to be less than 15 cm (Kääb, 2008).

### 3.4 Post-processing

All global elevation data sets used here are the result of the combination and post-processing of individual original data tiles, in particular SRTM (Rabus et al., 2003) and ASTER GDEM (METI/NASA/USGS, 2009). Among others, these procedures include vertical merging of overlapping elevations and horizontal mosaicking. These steps make the original sensor geometry inaccessible and thus prevent the physical modelling of errors and error propagation. Similar problems arise also for other elevation data sets such as from airborne laser scanning or aerophotogrammetry, but usually

## Correcting elevation data for glacier change detection

C. Nuth and A. Kääb

Title Page

Abstract

Introduction

Conclusions

References

Tables

Figures



Back

Close

Full Screen / Esc

Printer-friendly Version

Interactive Discussion



at much lower levels if proper strip overlaps/adjustments and aerotriangulation procedures are applied.

## 4 Methods

To minimize the significance level an elevation change requires for detection, we seek to analyze elevation differences on terrain assumed to be stable (e.g. not on a glacier) for 3 potential biases

1. the geo-location of the data (x, y, and z matrices),
2. an elevation dependent bias, and
3. biases related to the acquisition geometry of the data.

Some previous studies have searched for elevation biases and derived adjustments based upon multiple linear regressions between elevation differences with the terrain parameters (Gorokhovich and Voustianiouk, 2006; Racoviteanu et al., 2007; Peduzzi et al., 2010). Other studies have co-registered the DEM pairs, or derived products such as orthoimages, using image matching techniques, or 2-dimensional least squares regression (Berthier et al., 2007; Howat et al., 2008; Berthier and Toutin, 2008), or by providing a full co-registration solution of the translation, rotation and scale matrices (Gruen and Akca, 2005; Miller et al., 2009). Here, we choose to analyze each bias individually and present solutions for each of these iteratively, rather than combining all into one full regression or co-registration adjustment. The reason for that is to be able to follow and understand individual error terms, and to decide individually on their correction. Furthermore, it will become clear why a multiple regression based upon some combination of these terrain parameters will be significant, though such a correction may not be geometrically appropriate (e.g., see Peduzzi et al., 2010).

Elevation differences are here calculated by re-sampling the spatial resolution of one of the DEMs to the other, or in cases involving ICESat, interpolating the DEM at the

## Correcting elevation data for glacier change detection

C. Nuth and A. Kääb

Title Page

Abstract

Introduction

Conclusions

References

Tables

Figures



Back

Close

Full Screen / Esc

Printer-friendly Version

Interactive Discussion



estimated centroid of the ICESat footprint. Bi-linear interpolation is used in both cases. Determining which DEM should be re-sampled to the other is subjective and will vary for each study. However, this decision should be well considered as differences in the corrections may occur depending upon whether one samples to the larger pixel size or vice versa (Paul, 2008). It could be worthwhile to check corrections by re-sampling in each direction to determine such influences. In the case studies presented here, the oldest DEM is generally re-sampled to the newest DEM unless otherwise stated. We use the population of assumed stable terrain elevation differences to analyze the quality of the comparison. Glacier and water pixels/points are removed using land and glacier polygon masks. In New Zealand, the glacier masks are derived from ASTER imagery (Gjermundsen, 2007) while the ocean and lake boundaries were downloaded freely from GADM database of Global Administrative Areas (<http://www.gadm.org>) (GADM, 2010). In Svalbard, the glacier masks are a part of the new digital Svalbard glacier atlas which is soon to be released by the Norwegian Polar Institute. The ocean is masked using data from the Norwegian Polar Institute mapping department.

#### 4.1 A universal co-registration correction

Two DEMs of the same terrain surface that are not perfectly aligned experience a characteristic relationship between elevation differences and the direction of the terrain (aspect) that is precisely related to the x-y-shift vector between them. The relationship between elevation error and aspect has been described previously (Schiefer et al., 2007; Gorokhovich and Voustianouk, 2006; Peduzzi et al., 2010), although corrections applied in the latter two studies were not analytical but based upon multiple regression adjustments to elevation. Gorokhovich and Voustianouk (2006) showed the significance of the relationship between elevation differences and aspects on large slopes but overlooked the underlying cause as described in Kääb (2005).

The simplicity of this relationship and detection of unaligned DEMs lies in the similarity of elevation differences with the hillshade of the terrain (Fig. 1), a function that is based upon terrain slope and aspect. The correction of the mis-alignment requires

## Correcting elevation data for glacier change detection

C. Nuth and A. Kääb

Title Page

Abstract

Introduction

Conclusions

References

Tables

Figures



Back

Close

Full Screen / Esc

Printer-friendly Version

Interactive Discussion



a more detailed derivation. Figure 2 shows a schematic drawing and a real example where one DEM is shifted to the second DEM. Resulting elevation differences are larger on steeper slopes due to the relationship of the magnitude of the shift vector ( $\mathbf{a}$ ) and the elevation errors to the tangent of the slope of the terrain ( $\alpha$ ):

$$\tan(\alpha) = \frac{dh}{a} \quad (1)$$

Additionally, elevation differences are positive on eastern slopes and negative on western slopes, exemplifying the relationship of the differences to aspect ( $\Psi$ ). Because terrain aspect is usually defined circular from the north (azimuth), the direction of the shift can be modeled using a cosine of the difference between terrain aspect and the horizontal directional component of the shift vector. Combining this with the relation described by Eq. (1) derives the full analytical solution by relating the elevation differences to the elevation derivatives slope and aspect (Kääb, 2005):

$$dh = a \cdot \cos(b - \Psi) \cdot \tan(\alpha) + \overline{dh} \quad (2)$$

where  $dh$  is the individual elevation difference,  $b$  is the direction of the shift vector,  $\alpha$  is the terrain slope,  $\Psi$  is the terrain aspect and  $\overline{dh}$  is the overall elevation bias between the two elevation data sets. Slope and aspect can be calculated by any standard GIS or mathematical software, and different approaches exist depending upon application. In this case, the finite difference method is more appropriate than the D8 method (Wilson and Gallant, 2000). To remove the error dependency on slope due to an x-y shift, we normalize the vertical deviations by dividing by the tangent of slope at that pixel. This produces a very clean sinusoidal relationship between elevation difference and aspect (Fig. 2). The transformation of Eq. (2) after slope normalization is:

$$\frac{dh}{\tan(\alpha)} = a \cdot \cos(b - \Psi) + c \quad (3)$$

where

$$c = \frac{\overline{dh}}{\tan(\overline{\alpha})} \quad (4)$$

## Correcting elevation data for glacier change detection

C. Nuth and A. Kääb

Title Page

Abstract

Introduction

Conclusions

References

Tables

Figures

⏪

⏩

◀

▶

Back

Close

Full Screen / Esc

Printer-friendly Version

Interactive Discussion



Three cosine parameters ( $a$ ,  $b$  and  $c$ ) are solved using least squares minimization where the amplitude of the cosine ( $a$ ) is directly the magnitude of the shift vector,  $b$  is the direction of the shift vector and  $c$  is the mean bias between the DEMs divided by the mean slope tangent of the terrain (see Fig. 2). Because the solution to this actually analytical relationship is solved using the terrain which is not an analytical surface, the first solution may not be the final solution and iteration of the process is required to arrive at an ultimate solution. We choose to stop the iteration after the improvement of the standard deviation is less than 2% or if the magnitude of the solved shift vector is less than 0.5 m.

## 4.2 Elevation dependent correction

An elevation dependent bias can be commonly found within stereoscopic DEMs derived from optical satellite sensors (Berthier et al., 2004; Kääb, 2008). An elevation dependent bias can for instance result from an uneven spatial distribution of the GCPs in the x-y-z-planes which leads to a poorly resolved stereo orientation that could cause a distortion of the z-scale in the measurement of parallaxes. In these cases, either a linear or polynomial relationship between the elevation differences and elevation have been used to adjust the DEMs; e.g.:

$$dh = \sum_1^n (\kappa_n Z^n) + \tau \quad (5)$$

where  $Z$  is elevation,  $\kappa$  and  $\tau$  are the regression parameters and  $n$  is the order of the polynomial (e.g. 1 for linear). The range of previously applied linear corrections varies from 1 to 40 m per 1000 m (Berthier et al., 2007; Kääb, 2008; Berthier et al., 2010). Figure 3 shows an example between a 2003 and 2002 ASTER DEM (as described in Sect. 5) where a significant elevation dependent bias is apparent, which leads to a correction of  $\approx 10$  m per 1000 m (Table 2).

An elevation dependent bias is also suggested to exist within the SRTM over non-glaciated terrain (Berthier et al., 2006, 2007) and has been corrected for in some

## Correcting elevation data for glacier change detection

C. Nuth and A. Kääb

Title Page

Abstract

Introduction

Conclusions

References

Tables

Figures



Back

Close

Full Screen / Esc

Printer-friendly Version

Interactive Discussion



studies (Surazakov and Aizen, 2006; Schiefer et al., 2007), though this bias may also be the result of varying resolutions (see Paul, 2008). The SRTM is also expected to contain some bias due to penetration of the C and X Band radar waves into snow and ice which, has been suggested to be up to 10 m (Rignot et al., 2001). It is difficult to apply corrections for this type of bias since the snow/ice characteristics at the time of SRTM acquisition must be known.

Either way, an elevation dependent bias is extremely significant for estimating glacier volume changes because a glacier and its mass balance varies predominantly with elevation, and thus a bias with elevation either from failure of the z-scale or from radar wave penetration into snow/ice will directly affect the measurement and interpretation of either glacier thinning or thickening. Linear bias with elevation causes either over- or under- estimated elevation changes of a shrinking glacier depending upon whether the bias stems from the newest or oldest topography, respectively (Berthier et al., 2006).

### 4.3 Along/cross track corrections

While the above co-registration and elevation-dependent bias are in principle universal to all types of elevation data, additional individual error characteristics apply according to the sensor type and method used for DEM generation. Along/Cross track biases are the errors associated with the satellite geometry, and may only be relevant for satellite stereoscopic DEMs. Few studies demonstrate that such along/cross track error exists. Leprince et al. (2007) showed that an along track pattern with a frequency of 11–12 cycles per scene existed within the geo-location of pixels of an ASTER scene, corresponding to the 11–12 tie points where the Terra satellite acquires specific attitude information (ERSDAC, 2007). They relate this bias specifically to the under-sampling of the pitch information. Berthier et al. (2007) find elevation biases of a SPOT5 cross-track stereo DEM of up to 12 m which they can reproduce using the highly sampled attitude measurements, specifically the roll in this example. To analyze these errors, we rotate the coordinate system from X- and Y- to cross ( $X_{\text{track}}$ ) and along ( $A_{\text{track}}$ ) track directions, respectively, using a preliminary along track angle ( $\theta$ ) estimated from the

## Correcting elevation data for glacier change detection

C. Nuth and A. Kääb

Title Page

Abstract

Introduction

Conclusions

References

Tables

Figures



Back

Close

Full Screen / Esc

Printer-friendly Version

Interactive Discussion



two corners of available data in the scene:

$$A_{\text{track}} = X \sin(\theta) + Y \cos(\theta) \quad (6)$$

$$X_{\text{track}} = X \cos(\theta) - Y \sin(\theta) \quad (7)$$

Bias adjustments, if required, are fitted to these parameters using higher order polynomials, as described in the following sections. Section 5.3 provides an example of this bias and a correction using polynomials.

Errors related to the acquisition geometry is not restricted to stereo elevation data, but may also be present in interferometric DEMs. Height errors in InSAR generated DEMs generally derive from phase noise, atmospheric distortions and the imaging geometry (Knöpfle et al., 1998). In terms of geometry, the baseline length, along track position and platform height will all induce elevation errors within InSAR generated DEMs (Farr et al., 2007).

#### 4.4 Error propagation

Errors within elevation data, whether a DEM or individual points, are commonly estimated by comparing to independently acquired GCPs, generally of a much higher accuracy than that of the elevation source being tested. The quantification of this error, assuming the GCPs are absolutely correct, typically uses 2 measures of statistical spread of the residuals, the Root Mean Square Error (RMSE) or the standard deviation ( $\sigma$ ), assuming Gaussian distribution of the residuals (or perfect randomness). However, if the mean difference of the residuals does not equal zero, then the RMSE is not a proper estimate of the statistical error distribution, and the mean and standard deviation should be reported (Li, 1988; Fisher, 1998). In this study, we do not use GCPs for accuracy determination, but rather create a residual population of the difference between two independent data sources over stable terrain. These residuals represents the *relative* errors between elevation data sets, rather than *absolute*.

## Correcting elevation data for glacier change detection

C. Nuth and A. Kääb

Title Page

Abstract

Introduction

Conclusions

References

Tables

Figures



Back

Close

Full Screen / Esc

Printer-friendly Version

Interactive Discussion



Standard principles of error propagation are used for estimating errors between two DEMs (Burrough et al., 1998). For example, if one DEM has a random error,  $\sigma_1$ , and the second DEM,  $\sigma_2$ , then the resulting error of a statistically independent elevation difference point or pixel is defined as:

$$\varepsilon = \sqrt{\sigma_1^2 + \sigma_2^2} \quad (8)$$

However, elevation data, especially DEMs contain a degree of spatial autocorrelation that should be accounted for. The adapted error equation is then:

$$\varepsilon = \sqrt{\sigma_1^2 + \sigma_2^2 + 2 \cdot \sigma_1 \cdot \sigma_2 \cdot r} \quad (9)$$

where  $r$  is the correlation between  $\sigma_1$  and  $\sigma_2$  (Burrough et al., 1998; Etzelmüller, 2000). Determination of  $r$  requires semi-variogram analysis and advanced statistical procedures (Bretherton et al., 1999; Rolstad et al., 2009). When analyzing and quantifying glacier elevation changes, not just the spread of elevation changes is desired but rather the mean of the elevation changes over a particular area, e.g. a glacier or glacier zone. The standard error equation about the mean is defined (Davis, 2002),

$$S_\varepsilon = \frac{\varepsilon}{\sqrt{n}} \quad (10)$$

where  $n$  is the number of measurements. Two approaches to apply this equation to autocorrelated datasets are to use  $\varepsilon$  as defined in Eq. (9) or to use  $\varepsilon$  as defined in Eq. (8) and define  $n$  as the amount of un-correlated measurements. In the latter approach, some studies have assumed an autocorrelation distance of 500 m (Berthier et al., 2010) or 1 km<sup>2</sup> (Nuth et al., 2007; Kääb, 2008).

#### 4.5 Estimating the geodetic balance and its errors

There are two approaches for integrating glacier elevation changes into a volume change. The first is to apply the *grid* method by summation of all the differential DEM

### Correcting elevation data for glacier change detection

C. Nuth and A. Kääb

Title Page

Abstract

Introduction

Conclusions

References

Tables

Figures



Back

Close

Full Screen / Esc

Printer-friendly Version

Interactive Discussion



pixels over the glacier multiplied by the pixel resolution (e.g. Etzelmüller, 2000; Kohler et al., 2007; Paul and Haeberli, 2008; Berthier et al., 2010):

$$dV = \sum_1^n (dh) \times r^2 \quad (11)$$

where  $dV$  is the volume change,  $r$  the resolution and  $n$  is the number of pixels. The second method is to use a *hypsometric* approach where an elevation change by elevation relationship is multiplied by the hypsometric area ( $A_z$ ) of the glacier basin (e.g. Arendt et al., 2002; Berthier et al., 2004; Kääb, 2008; Nuth et al., 2010):

$$dV = \sum_1^z (\overline{dh}_z \cdot A_z) \quad (12)$$

where  $\overline{dh}$  can either be the mean or median in elevation bins, or a polynomial model of the elevation changes as a function of elevation. Equation (12) assumes normality of the changes over an elevation bin. Situations in which the glacier has multiple upper basins behaving differently may lead to failure of the assumption. In this study we will define the geodetic balance as the annual average volume change per area. For the *grid* method, this is the average of the glacier elevation change pixels. For the *hypsometric* method, the volume change is divided by the total area. In both approaches, the geometry remains fixed (reference mass balance) which will be slightly more negative than the hydrologic mass balance of a retreating glacier (Elsberg et al., 2001).

We will calculate annual geodetic balances using both approaches and therefore derive error equations for each approach by making adaptations to Eqs. (8) and (10). The error equation for the *grid* method is:

$$\varepsilon_1 = \sqrt{\frac{\sigma_1^2 + \sigma_2^2 + \sigma_g^2}{N_m}} \quad (13)$$

## Correcting elevation data for glacier change detection

C. Nuth and A. Kääb

Title Page

Abstract

Introduction

Conclusions

References

Tables

Figures

◀

▶

◀

▶

Back

Close

Full Screen / Esc

Printer-friendly Version

Interactive Discussion



And that for the *hypsometric* method is:

$$\varepsilon_2 = \sqrt{\sum_1^z \left[ \sqrt{\frac{\sigma_1^2 + \sigma_2^2 + \sigma_g(z)^2}{N_m(z)} \times \frac{A(z)}{A_{\text{total}}}} \right]^2} \quad (14)$$

where  $\sigma_g$  is the standard deviation of glacier elevation changes,  $A$  is the area,  $z$  are the elevation bins, and  $N_m$  is the number of un-correlated measurements. Equation (13) varies from Eq. (10) in that an additional term,  $\sigma_g$ , is added to account for the representativeness of the mean ice elevation change. Equation (14) is different from Eq. (13) in that it includes weights based upon the hypsometric distribution of the glacier. Equation (14) also assumes that the estimation of each elevation bin of a glacier is independent, which may not be the case, especially when local systematic errors are present. Therefore, this error derivation assumes that all systematic biases have been removed from the dataset. In this study, we will assume an auto-correlation length of 1 km. All error estimates in this study are divided by the time between DEMs to convert them into annual estimates.

The conversion between volume and density is ignored in this study because the main focus is on errors within the DEMs. Common practice is to apply Sorge's Law (Bader, 1954) and multiply by the density ratio of ice to water (0.9). Other studies have adapted either a lower density related to the density of firn and the accumulation area ratio (Sapiano et al., 1998; Hagg et al., 2004), or a zonal or elevation dependent conversion (Moholdt et al., 2010b).

## 5 Case Study 1: New Zealand

### 5.1 Global data sets

Three publicly available nearly global elevation datasets, the SRTM DEM, ICESat and the ASTER GDEM are compared against each other. All three datasets are

2030

## Correcting elevation data for glacier change detection

C. Nuth and A. Kääb

Title Page

Abstract

Introduction

Conclusions

References

Tables

Figures

◀

▶

◀

▶

Back

Close

Full Screen / Esc

Printer-friendly Version

Interactive Discussion



well oriented to each other at the regional scale. The universal correction of ASTER GDEM to ICESat and the SRTM both resulted in a 10 m shift to the Northwest direction. The shift between SRTM and ICESat was less than a meter. A triangulation of these three shift vectors resulted in error residuals less than 0.3 m in the x and y directions, and  $\approx 1.5$  m in the z-direction (triangulating residuals is described in more detail in Sects. 5.3 and 6.1). However in this case, the solution for the shifts are completely dependent upon the size of the area chosen for analysis. Both the ASTER GDEM and the SRTM products are compiled of many images and overlaying acquisitions and therefore may contain shifts in varying directions within different areas. Figure 4 shows normalized histograms of the elevation differences between the three data products after co-registration. The standard deviation between the SRTM and ICESat is  $\approx 5$  m whereas the standard deviation between the ASTER GDEM with SRTM and ICESat is twice that,  $\approx 10$  m.

## 5.2 The ASTER GDEM

The statistics presented above about the ASTER GDEM are similar to those from the validation summary (METI/NASA/USGS, 2009) with biases of up to 10 m and RMSE of 5–50 m. However the report states, “that the ASTER GDEM does contain residual anomalies and artifacts that most certainly degrade its overall accuracy, represent barriers to effective utilization of the GDEM for certain applications, and give the product a distinctly blemished appearance in certain renditions” (METI/NASA/USGS, 2009). The sources for the artifacts are residual cloud blemishes and the algorithm used to compile and generate the final DEM, the latter which is of most significance. Nonetheless, METI/NASA released this product publicly as an *experimental/research* grade product in hopes to derive a better Global DEM in the future.

Analysis of the spatial distribution of the elevation differences between SRTM and the GDEM reveal large-scale linear features (Fig. 5) which are highly related to the number of images used in the GDEM for a specific location (METI/NASA/USGS, 2009). Consistent bias persists over distances of 10–20 km with multiple slightly sinusoidal patterns

### Correcting elevation data for glacier change detection

C. Nuth and A. Kääb

Title Page

Abstract

Introduction

Conclusions

References

Tables

Figures



Back

Close

Full Screen / Esc

Printer-friendly Version

Interactive Discussion



of amplitudes of up to 10–20 m. The implications of these large-scale linear features present within the GDEM infer that bias of individual ASTER scenes is incorporated into the GDEM. This bias can be quite significant and we hypothesize that it has roots within the original DEM generation and merging of the ASTER scenes. Simple inspection of the false hillshade (as shown in Fig. 1) of the elevation differences between the GDEM and SRTM reveal the multiple directional shifts within the product.

In terms of glaciological research, the GDEM may be an appropriate data source for deriving area-altitude distributions of glaciers which can be useful for volume change estimation using ICESat (Moholdt et al., 2010b) or for providing elevation input data required for spatial mass balance modelling. However, the GDEM is not appropriate for change detection because of the numerous artifacts present within the data and the lack of a time stamp for individual pixels. Thus, the next section provides an analysis of ASTER DEMs from individual scenes in order to determine the appropriateness of these data to detect glacier changes.

### 5.3 Individual ASTER DEMs

This section refers to individual ASTER DEMs as computed by LPDAAC using the SilcAst software and onboard-derived orientation parameters only (no GCPs; ASTER product AST14). Before calculating glacier elevation changes, we compare each possible combination of the data in Table 1 producing 10 differential DEMs. The population is first filtered using a  $3\sigma$  filter which removes the largest outliers. For each DEM pair, three potential adjustments are applied iteratively using the population of stable terrain difference pixels:

1. Co-register the DEMs using Eq. (3). Practically, we solve for the parameters ( $a$  &  $b$ ) iteratively until the improvement of the standard deviation is less than 2%. We convert each iteration of the magnitude ( $a$ ) and angle ( $b$ ) of the shift vector into its  $x$ - and  $y$ - components using trigonometry and sum up the iterations to determining the final adjustment that is applied either on the corner coordinates or the  $x$  and  $y$

## Correcting elevation data for glacier change detection

C. Nuth and A. Kääb

Title Page

Abstract

Introduction

Conclusions

References

Tables

Figures



Back

Close

Full Screen / Esc

Printer-friendly Version

Interactive Discussion



**Correcting elevation data for glacier change detection**

C. Nuth and A. Kääb

[Title Page](#)[Abstract](#)[Introduction](#)[Conclusions](#)[References](#)[Tables](#)[Figures](#)[⏪](#)[⏩](#)[◀](#)[▶](#)[Back](#)[Close](#)[Full Screen / Esc](#)[Printer-friendly Version](#)[Interactive Discussion](#)

vectors of one of the DEMs.

2. Search and adjust for any elevation dependent bias. We use a robust regression of the elevation differences with elevation to solve Eq. (5) which is then used to correct one of the DEMs.

3. Search for any bias related to the acquisition geometry of the ASTER satellite. Here we search for biases that occur in the along and cross track directions of the satellite overpass. Higher order polynomials (6th to 8th order) are then fit to the elevation differences with along/cross track directions which is used to adjust one of the DEMs.

Table 2 shows the results for each DEM pair before any adjustments are applied and after each correction is applied iteratively. In total, the three corrections improve the standard deviation of stable terrain from 8–69%. The most significant improvement is obtained through co-registration of the DEM pair. Each individual ASTER DEM has a unique linear x-, y- and z-bias to the SRTM, independent of any other scenes. The direction of the shift is not uniform for all scenes which has important repercussions on the quality of the algorithms used to create the ASTER GDEM.

The most significant elevation dependent bias corrections occur in the 2001 and 2003 scenes where the corrections are as much as 10 m per 1000 m. In these scenes, the ocean covers  $\approx 30\%$  making the potential distribution of automatically generated tie points not uniformly distributed in space. Whether this refinement is performed within the DEM generation is not completely known to us, though it may provide an explanation to why these scenes contain large elevation scale distortions. Alternatively, the 2002 and 2006 scenes do not contain any ocean or significant distortions. However, an elevation dependent bias may be confounded with biases related to the sampling resolution (Paul, 2008). We test this on the 2001 and 2003 scenes by taking the inverse differences, i.e. resampling the ASTER to the 90 m SRTM DEM. We find that the slope of the elevation dependent bias does not change significantly though slightly smaller.

## Correcting elevation data for glacier change detection

C. Nuth and A. Kääb

Title Page

Abstract

Introduction

Conclusions

References

Tables

Figures



Back

Close

Full Screen / Esc

Printer-friendly Version

Interactive Discussion



In 9 out of 10 cases, the along/cross track corrections improved the standard deviation of elevation difference residuals. It may be questionable whether this bias is significantly determined or not. For example, the 2001 and 2003 scenes in this study contain  $\approx 30\%$  ocean, and thus the spatial distribution of terrain differences are not uniformly distributed in the along and cross track directions. In these scenes, the cross track direction is undersampled where the along track correction is completely sampled, and vice versa, which leads to overcompensation in either end of the along/across track corrections. However, in the following paragraphs we discuss two examples that show that this bias can have important repercussions on the elevation differences further warranting a correction.

Figure 6 shows the processing sequence for differencing the 2006 ASTER DEM to the SRTM which we take to be the reference surface. About 20% of the ASTER scene is covered by semi-transparent clouds that result in erroneously high elevations in the DEM. These extremes are effectively removed by  $3\sigma$  filters on the elevation differences. Figure 6a and b shows the original elevation differences and their relationship with aspect which results in a shift vector of 30 m to the northeast. The elevation-dependent bias is not significant enough to warrant a correction (see Table 2). After shifting (Fig. 6c), a visible pattern remains related to the along/cross track directions (Fig. 6d and e). We fit 8th and 6th order polynomials to the differences in the along/cross track direction, respectively, and adjust first along track before re-calculating the cross track correction. The two adjustments applied to the ASTER DEM (1st – Shifting, 2nd – Along/Cross track) resulted in a 35% and 6% improvement in the standard deviation, respectively, which can be seen in the elevation difference histograms of Fig. 6g. The final RMSE between the ASTER DEM and SRTM is 10.6 m, down from an original RMSE of 18 m.

Another interesting example is the difference between the 2006 and 2002 ASTER SilcAst DEMs. A shift of  $\approx 45$  m in a NE-SW direction is observed and corrected (Fig. 7a). An elevation dependent bias showed not more than  $\approx 1$  m per 1000 m which we do not correct for. Slight along/cross track biases are present up to  $\pm 5$  m that are corrected

using a 6th order polynomial (Fig. 7b and c). The post-correction pattern of elevation difference (Fig. 7d) reveal linear cross track striations that run along track of the flight path of the ASTER scene. These features are similar to the linear features discovered by Leprince et al. (2007) which they relate to *jitter* of the instrument and under-sampling of the sensor attitude information in the along-track direction (specifically, the pitch). In particular, the geometric correction of the ASTER images relies on a lattice of 12 by 11 points along/cross track, respectively, where precise satellite attitude measurements are acquired. A linear interpolation is used for geolocating all pixels in between these lattice points (ERSDAC, 2007). The number of cycles apparent in the mean vertical differences along track (Fig. 6d) is  $\approx 10$ –12 cycles. The vertical amplitude of these variations is  $\pm 2$  m giving a full range of 4 m. We choose not to correct for this bias as it is below the significant level of our dataset. However, if an extremely *precise* DEM is available (e.g. laser scanning), these higher frequency bias corrections will probably be above the significance level.

This example both shows that along/cross track biases exist within the DEMs, and that corrections can be applied with relatively good confidence. We find that along/cross track bias seems to occur at 2 levels of frequency. A lower frequency pattern with generally 2–3 cycles within an ASTER scene is the most significant with an amplitude of up to 5 m. The higher frequency variability occurs with  $\approx 10$ –12 cycles per scene. The visibility of this higher frequency error confirms the appropriateness of our lower frequency correction. The unrecorded pitch variations which are the hypothesized cause of the higher frequency bias occur independently for each scene acquisition. They are integrated into the DEM creation, most likely during the back-looking pass of the satellite because small variations (*jitter*) in the back-looking pitch cause slight variations in the looking angle directly affecting the vertical component of the parallax estimates. In this case, the unrecorded pitch variations of both stereo-pairs seem to have been in opposite directions and overlaid each other constructively (i.e. added to each other) as otherwise the vertical variations would vanish (i.e. destructive superposition).

## Correcting elevation data for glacier change detection

C. Nuth and A. Kääb

[Title Page](#)[Abstract](#)[Introduction](#)[Conclusions](#)[References](#)[Tables](#)[Figures](#)[◀](#)[▶](#)[◀](#)[▶](#)[Back](#)[Close](#)[Full Screen / Esc](#)[Printer-friendly Version](#)[Interactive Discussion](#)

For detecting glacier elevation changes, the most important correction is shifting the two DEMs to each other (co-registration). The universal co-registration correction can be solved for each DEM pair and the combination of three correction vectors (from 3 DEMs) can derive residuals, for example;

$$Z_{13} = Z_{12} + Z_{23} \quad (15)$$

where  $Z_{12}$  is the correction vector from DEM 1 to 2 etc., but can also be the elevation difference matrices themselves. The residuals reflect the internal accuracy or coherence between the three data sets or correction vectors. All 5 datasets (SRTM + 4 ASTER DEMs) are compared providing 10 residuals (Table 3). The standard deviations for the length of the 3 component residual vectors is  $\approx 4$  m. The shift solution has an internal horizontal accuracy of at least  $1/3$  of an ASTER DEM pixel (30 m), though often  $1/10$  of a pixel. The nominal vertical accuracy lies around 1–2 m, though 4–5 m in worst case scenario. Therefore in this example, a glacier must have more than 4 m of change to detect an elevation change and greater than at least 8 m to detect an elevation change that may not be 50% biased. The glacial implications is that the longer the time difference between the two DEMs, the smaller impact the bias has on annual averaged elevation change rates. The approach of residual triangulation of the shift vectors is also an effective way to detect erroneous or less significant shifts. It may also be used with elevation change matrices to determine if a time series is internally consistent after shifting and/or if any less significant along/cross track corrections applied have introduced vertical biases. The mean and standard deviations of the population of triangulated elevation change residuals reflects slightly the residuals of the vertical component and the total length of the shift vectors ( $\varepsilon_Z$  and  $\varepsilon_{r_{SS}}$ ), respectively (Table 3).

An artifact in differential DEMs that involve the SRTM DEM and that we do not correct for is the penetration of radar waves into snow and firn (König et al., 2001). The SRTM DEM used here is derived from C-band radar (center frequency at 5.3 GHz). Rignot et al. (2001) determined that the phase center of the C-band signal return was 1 to 10 m into the surface depending upon the snow conditions (i.e. dry vs. wet) in Greenland and

## Correcting elevation data for glacier change detection

C. Nuth and A. Kääb

[Title Page](#)[Abstract](#)[Introduction](#)[Conclusions](#)[References](#)[Tables](#)[Figures](#)[⏪](#)[⏩](#)[◀](#)[▶](#)[Back](#)[Close](#)[Full Screen / Esc](#)[Printer-friendly Version](#)[Interactive Discussion](#)

Alaska. In Svalbard, the volumetric phase center of the C-band varied from  $\approx 1$  to 5 m along a profile from ablation to firn zones, respectively (Müller et al., 2010). Corrections for depth penetration are hardly used for the SRTM data, and is extremely difficult to correct for as knowledge of the snow conditions at the time of acquisition is required yet hardly available. Nonetheless, one should be aware of this bias, especially when using the SRTM to produce elevation changes over short time scales (as shown later).

## 5.4 Glacier elevation changes

We analyze four glaciers in the NZ Southern Alps, all located around Mt. Cook: Franz Joseph, Fox, Tasman and Murchison glaciers. They are the four largest glaciers in New Zealand, but vary in their mass balance characteristics, and thus their dynamical response times. The glaciers on the west (Franz Joseph and Fox) have large amounts of accumulation and ablation (Anderson et al., 2006) as compared to the glaciers on the east of the divide due to a large east-west precipitation gradient (Fitzharris et al., 1999) and are generally quite steep, with rather short response times (Oerlemans et al., 2005). The glaciers on the east side of the divide (Tasman and Murchison) have debris covered tongues with less accumulation and ablation (Kirkbride, 1995). This glacier variation between the east/west glaciers allow for an interesting comparison related to the significance an elevation change requires for adequate detection.

The detection of glacier elevation changes is dependent upon both glacier characteristics and data precision. Assuming an accuracy of  $\pm 15$  m for each ASTER SilcAst DEM (i.e. the standard deviation of terrain differences presented in Sect. 5.3), the error associated with an individual difference pixel is  $\pm 21$  m (using Eq. 8) for a single year DEM difference and  $\pm 3.5$  m yr<sup>-1</sup> for a 6 year difference. Therefore, mainly glacier changes on the tongue are significantly different than zero.

For both east coast glaciers, the here-estimated rate of frontal thinning is  $\approx 3$ – $4$  m yr<sup>-1</sup> between 2000 and 2002 and  $\approx 1$ – $2$  m yr<sup>-1</sup> between 2002 and 2006. The most significant elevation changes measured are within the longest time period, 2000–2006, which show frontal thinning between 1 and 4 m yr<sup>-1</sup>. These rates compare well with

## Correcting elevation data for glacier change detection

C. Nuth and A. Kääb

Title Page

Abstract

Introduction

Conclusions

References

Tables

Figures

◀

▶

◀

▶

Back

Close

Full Screen / Esc

Printer-friendly Version

Interactive Discussion



the longer term averages of  $\approx -1 \text{ m yr}^{-1}$  between 1890–1964/1971 (Skinner, 1964; Hochstein et al., 1995) as well as with a shorter term average frontal thinning between 1987 and 2007 of  $\approx 4.5 \text{ m yr}^{-1}$  (Quincey and Glasser, 2009). It is apparent in the 2000 to 2006 changes of Fig. 8 that Murchison glacier experiences more negative frontal thinning than the Tasman glacier. However, over these short time periods local bias may produce significant artifacts. We also attempted to calculate single year elevation changes between the ASTER SilcAst DEMs. However, the changes showed no coherent relationship with elevation, but rather looked like random noise. In summary, the small changes of these glaciers east of the divide would thus require a longer time period between DEMs than shown here to derive significant changes above the noise threshold induced by both random and systematic errors.

Figure 9 shows elevation change rates of the glaciers on the west side of the divide. The changes on these glaciers are large enough that detection of elevation changes within a single year is possible. The tongue of Fox glacier showed up to 20 m thickness losses from 2000 to 2001 (Fig. 9), similar to the annual melt measured at the front of Franz Joseph Glacier (Anderson et al., 2006; Purdie et al., 2008). From 2001 to 2002, the tongue experienced vertical increases of 7–10 m, which implies a glacier advance while at the same time the upper glacier basins decreased slightly ( $\approx 1\text{--}5 \text{ m}$ ). Interestingly, if we did not use the 2001 data, and simply compared 2000 to 2002, we would have measured a comparably stable glacier with thickness losses of up to  $5 \text{ m yr}^{-1}$ . After 2002, the glacier seems to have continued to advance. Front position observations reported in the WGMS Fluctuations of Glaciers (WGMS, 2008) document a retreat from 2000–2001, a stable front from 2001–2002, retreat from 2002–2004 and an advance from 2004–2005. These observations neither agree or disagree with our findings, as thickness increases may or may not reach the front position, at least in cases of partial surges (Sund et al., 2009). It is difficult to conclude without any first-hand confirmation of thickening whether the increases between 2001 and 2002 is due to local biases within the ASTER scenes. Nonetheless, the longer period comparisons (2002–2006 and 2000–2006) show frontal thickening of  $\approx 5\text{--}10 \text{ m yr}^{-1}$ , and are less

## Correcting elevation data for glacier change detection

C. Nuth and A. Kääb

Title Page

Abstract

Introduction

Conclusions

References

Tables

Figures



Back

Close

Full Screen / Esc

Printer-friendly Version

Interactive Discussion



susceptible to noise and error as can be seen by the smoother elevation change fields in Fig. 9.

Annual elevation changes measured on Franz Joseph glacier are however plagued by noise and bias. In particular, an artificial mountain at the front of the glacier is apparent in most of the SilcAst DEMs as a result of matching failure. This artifact is removed by  $3\sigma$  filtering and explains why the front of the glacier is missing on most of the images in Fig. 9. The multi-annual measurements are smoother and less plagued by bias than the annual measurements. From 2000 to 2002, Franz Joseph seems to have thinned by  $\approx 5\text{--}10\text{ m yr}^{-1}$ , though since 2002, the tongue thickened by about  $5\text{ m yr}^{-1}$ . These results are consistent with the neighboring Fox glacier which experiences similar elevation changes, even though the WGMS reports frontal retreats of 20 to  $90\text{ m yr}^{-1}$  (WGMS, 2008). In conclusion, single year elevation changes were large enough on Fox glacier to permit significant detection of thickness changes, though the single year changes are the most susceptible to local biases that exist within the DEMs. Over multiple years, however, the signal-to-noise ratio between real elevation changes and the transported bias from DEM differencing is increased when computing annually averaged elevation change rates.

To complete this case study, total volume changes and associated geodetic balances are derived by applying both methods for estimating the geodetic balance (Eqs. 11 and 12) and the associated errors (Eqs. 13 and 14) for the four glaciers. Only estimates from 2000–2006 are presented because of the decreased sensitivity to bias, and despite the known penetration bias of the 2000 SRTM data. The DEM pair is co-registered and adjusted for along/cross track biases; elevation dependent bias was not considered significant. All estimates are in ice equivalent. Both Tasman and Murchison glaciers have negative geodetic balances. On Tasman glacier, Eqs. (11) and (12) result in an annually averaged estimate of  $-0.56 \pm 0.16$  and  $-0.42 \pm 0.22\text{ m yr}^{-1}$ , respectively. On Murchison, the geodetic balance estimates are  $-1.42 \pm 0.30$  and  $-1.10 \pm 0.35\text{ m yr}^{-1}$ , respectively. Fox glacier has a slightly less negative balance of  $-0.35 \pm 0.26$  and  $-0.35 \pm 0.33\text{ m yr}^{-1}$  for Eqs. (11) and (12), respectively. Franz Joseph glacier was

## Correcting elevation data for glacier change detection

C. Nuth and A. Kääb

Title Page

Abstract

Introduction

Conclusions

References

Tables

Figures



Back

Close

Full Screen / Esc

Printer-friendly Version

Interactive Discussion



not estimated because of the missing data at the glacier front. The variation between the two methods for volume change and geodetic balance estimates may be the result of outliers and non-normality of the elevation changes on a glacier. The error derivation using Eq. (14) is larger in all cases than that derived from Eq. (13). We believe that the hypsometric error method (Eq. 14) is probably a more reasonable error estimate, disregarding the inclusion of systematic bias.

The sensitivity of total volume change measurements to the bias adjustments is complex because of its dependence on both whether the bias occurs in the newer or older dataset as well as the direction (positive or negative) and magnitude of the bias in relation to the glacier hypsometry (Berthier et al., 2006). The results are further difficult to analyze because the biases are generally scene (or study) dependent. The alpine glaciers in this study, and in most of the world, contain bottle-neck geometries which means the majority of the glacier area is at higher elevations where elevation changes are typically below or at the significance level depending upon the time period the changes are being calculated. Because we assume that there should be less change at higher elevations, a volume change estimate from DEM differencing of a bottleneck glacier may be highly sensitive to these bias adjustments. Therefore, it is stressed that the error estimates defined here are for situations containing only random errors, and we are not completely sure that all systematic biases have been completely removed. Therefore, such short term geodetic estimates should be considered with precaution. However, the longer the time between DEMs, the less the sensitivity of these types of measurements to scene bias because of the greater signal-to-noise ratio.

## 6 Case study 2: Svalbard

The archipelago of Svalbard contains  $\approx 34\,000\text{ km}^2$  of glaciers, about 60% of the land area. The availability of stable terrain is limited to nunatak areas between the glaciers and the strandflats around the coastline (Hisdal, 1985). A 2003 ASTER SilcAst DEM is tested against a 2008 SPOT5-HRS DEM from the IPY-SPIRIT Project (Korona et al.,

### Correcting elevation data for glacier change detection

C. Nuth and A. Kääb

Title Page

Abstract

Introduction

Conclusions

References

Tables

Figures



Back

Close

Full Screen / Esc

Printer-friendly Version

Interactive Discussion



2009), a 1990 aerophotogrammetric DEM from the Norwegian Polar Institute (description and accuracy of the dataset can be found in Nuth et al., 2007, 2010) and 2003–2008 ICESat data (Table 4). The 1990 dataset is partially incomplete with a missing strip over the center of the ASTER scene. This has little repercussions besides the along/cross track adjustments described in Sect. 6.2. The landform characteristics within the ASTER scene is  $\approx 65\%$  glacier, 10% stable terrain and 25% ocean. The objective of this case-study is to demonstrate the ability of the universal co-registration correction and other bias adjustments in regions where stable terrain is severely limited, typical of the higher latitude glaciated regions.

## 6.1 Universal co-registration correction

We begin our 2nd case study by showing an example of the vertical differences before and after adjusting the ASTER SilcAst DEM to the SPOT5-HRS DEM (Fig. 10). Before adjustment, a distinct sinusoidal relationship between the vertical deviations and aspect is rather strong (Fig. 10) resulting in a shift of 75 m to the west-north-west ( $\approx 2.5$  ASTER pixels). The final fit solution was obtained after 3 iterations as opposed to 2 iterations common for all the ASTER DEMs tested in New Zealand. We additionally tested the two DEMs generated from the ASTER scenes acquired directly before and after the acquisition of the scene in Fig. 10. The shift vectors for these were all in the same direction and magnitude (not shown here).

The four datasets (Table 4) allow the derivation of 6 shift vectors (Table 5). The aerophotogrammetric DEM and ICESat (**DI**) resulted in the smallest shift vector ( $\approx 3$  m) and an RMSE (3.6 m) of stable terrain after two iterations. We expect the aerophotogrammetric DEM to be of the highest quality and accuracy, thus the impressive coherence with ICESat further confirms previously published ICESat horizontal and vertical accuracies (Fricker et al., 2005; Luthcke et al., 2005; Magruder et al., 2005; Brenner et al., 2007). For the other 5 comparisons, the SPOT5-HRS DEM compared better than the ASTER, with a shift vector solution, **SD** and **SI**, of  $\approx 20$  m ( $\frac{1}{2}$  pixel) and an RMSE of 8 and 5 m, respectively. All 3 shifts for the ASTER SilcAst (**AD**, **AS**, **AI**)

## Correcting elevation data for glacier change detection

C. Nuth and A. Kääb

Title Page

Abstract

Introduction

Conclusions

References

Tables

Figures



Back

Close

Full Screen / Esc

Printer-friendly Version

Interactive Discussion



resulted in vector magnitudes of 80–100 m, or  $\approx 2\text{--}3$  times the pixel size. The vertical RMSE for the ASTER DEMs is within the reported range, about 15–20 m for the three comparisons.

The shift vector magnitudes for ASTER (2–3 pixels) is much larger than that of SPOT ( $\frac{1}{2}$  pixel) in reference to ICESat and the aerophotogrammetric DEM, which reflects the more accurate satellite positioning and sensor pointing information of the SPOT5-HRS sensor as compared to ASTER. The elevation difference RMSE of the ASTER SilcAst products are double ( $\approx 20$  m) those from the SPOT comparison to the aerophotogrammetric DEM or ICESat. This mainly reflects the different spatial image resolution, but presumably also the different stereo configuration (forward-backward) of the SPOT5-HRS sensor with a base-to-height ratio of 0.8 that provides a more precise parallax measurement than the nadir-backward configuration of ASTER (base-to-height ratio of 0.6). The results in Table 5 suggest also that the cross-track positioning is less accurate than the along-track positioning.

Despite the spatial limitation of ICESat to ascending and descending tracks, it may still be used as a reference for any relative DEM, given a large enough distribution of points over stable nunataks. Schenk et al. (2005) showed the feasibility of using ICESat as ground control for historical vertical imagery and complimentary aerophotogrammetric DEMs by selecting visible nunatak areas and minimizing the vertical deviations of these areas through a 2-dimensional regression. Figure 11 shows the first iteration for the comparison of ASTER to the aerophotogrammetric DEM (**AD**) and to ICESat (**AI**). The sinusoidal relationship in both graphs are similar, though the variation in the relationship between **AI** is much larger due to the smaller sample size (less than 600 pts) of available stable terrain ICESat footprints (Table 5).

The internal consistency of the universal co-registration correction is tested by triangulating the shift vectors presented in Table 5. From the 4 elevation products and 6 shift vectors available between them, four error vectors can be calculated (Table 6). The lowest errors occur between the combinations SDI and ASD with horizontal positioning errors of less than 5 m whereas larger errors of  $\approx 10$  m occurs in the combinations

## Correcting elevation data for glacier change detection

C. Nuth and A. Kääb

Title Page

Abstract

Introduction

Conclusions

References

Tables

Figures



Back

Close

Full Screen / Esc

Printer-friendly Version

Interactive Discussion



ADI and AIS (Table 6). This difference is mainly caused by one poorly defined shift vector, **AI**. Figure 11 shows that the ASTER to ICESat comparison is noisier due to a smaller sample size ( $\approx 600$ ) and spatial distribution of stable terrain elevation points. The solution to Eq. (3) is weaker than other solutions involving ICESat; for example, **SI** contain more than 6000 stable terrain elevation differences and the distribution of these differences with aspect are a lot more uniform than that of **AI** (Fig. 11b). Nonetheless, despite the limited number of points, the correction to ICESat was still as precise as  $1/3$  an ASTER pixel (Table 6).

## 6.2 Glacier elevation changes

Svalbard glaciers, as opposed to New Zealand glaciers have much lower rates of ablation and accumulation. The elevation change rates of the previous decades are typically between  $-3$  and  $+1 \text{ m yr}^{-1}$  (Nuth et al., 2010; Moholdt et al., 2010b). Thus along track and cross track biases of up to 10 m as found in New Zealand will have a significant impact on any differences derived from less than 10 years. Other patterns of bias seem apparent within Fig. 10. To analyze these, we use ICESat acquisitions from the same year as the DEM acquisitions. One repeat track from 10 October 2003 and 3 March 2008 was available that is similar to the along track direction of the ASTER satellite overpass and contain a minimal cross-track separation (less than 15 m). The comparisons between the ASTER and SPOT5-HRS DEMs with the ICESat profiles is shown in Fig. 12. Despite the extreme limitation of stable terrain throughout the ASTER scene, we detect an along track bias of up to  $\pm 10$  m between the ASTER and SPOT5 DEMs shown in Fig. 12a. The differences between the ASTER and the 2003 ICESat track (Fig. 12d) is similar to the along track bias. No along track biases are seen between the ICESat track and the SPOT5 DEM. The slightly negative mean difference is probably a summer melt signal, especially significant in the first 5 km of the profile which ascend the front of Storbreen glacier with an apparent 5 month loss of  $\approx 2\text{--}2.5$  m (Fig. 12d). After correction, the 2008–2003 differences between the DEMs is similar to the ICESat to ICESat repeat track differences. This example proves the significance

## Correcting elevation data for glacier change detection

C. Nuth and A. Kääb

Title Page

Abstract

Introduction

Conclusions

References

Tables

Figures



Back

Close

Full Screen / Esc

Printer-friendly Version

Interactive Discussion



and feasibility of such corrections to the ASTER DEMs, even for situations when only a limited dataset of stable terrain (less than 10% of the scene) distributed unevenly over the scene is available.

Corrections of the along/cross track biases seem to remove most of the spatially visible trends between the ASTER and SPOT (Fig. 13). We use the same along/cross track corrections to difference the 2003 ASTER DEM with the 1990 aerophotogrammetric DEM because the missing strip in the 1990 data may weaken the significance of along/cross track biases. The mean bias between the adjusted 2003 ASTER DEM and the 1990 DEM ( $-0.7$  m) is therefore corrected. We denote a number of significant anomalies and glacier trends within Fig. 13. First, large bias anomalies are present towards the edges of the scene [**A** and **B**] as well as blunders from low cloud anomalies [**C**] that infect the entire southwestern coast of the image. Given the lack of a correlation and/or cloud mask for the automatically generated ASTER DEMs, these blunders remain difficult to remove, and must be masked manually.

In terms of glacier changes, it is clearly visible that the 1990–2003 changes are smoother and less plagued by random noise and bias as in the 2003–2008 differences (Fig. 13). This is purely the effect of time difference between the DEMs. Other glacier anomalies apparently include the surges of Zawadskibreen [**Z**], Dobrowlskibreen [**Db**] and Perseibreen [**P**]. Zawadskibreen shows large losses of  $\approx 30$  m in the southeastern cirque with slight increases of  $+10$  m along the central flow-line at 400 m a.s.l. The initiation of this surge could have been anytime between 1990 and 2003, though first visible signs appeared in the 2003 ASTER (Sund et al., 2009). After 2003, the progression of the surge is clearly visible where about 10–20 m losses are seen above 400 m a.s.l. and about 50–60 m increases towards the surge bulge at 200 m a.s.l. The surge of Dobrowlskibreen is clearest in the 1990–2003 differences with increases at the confluence with Nathorstbreen [**N**]. The 2003–2008 differences however show continued losses at the higher elevations, with little to no thinning at the lower elevations. The bulk of the surge of Perseibreen occurred during 2000–2001 with 3 month summer average speed of  $\approx 3$  m d<sup>-1</sup> (Dowdeswell and Benham, 2003). The large geometric

## Correcting elevation data for glacier change detection

C. Nuth and A. Kääb

Title Page

Abstract

Introduction

Conclusions

References

Tables

Figures



Back

Close

Full Screen / Esc

Printer-friendly Version

Interactive Discussion



change of the glacier is clearly seen between 1990–2003, despite the missing 1990 data in the upper cirque regions. Since 2003, the glacier continued to thin at higher altitudes with losses of up to 50 m in the western cirque. Slight increases occurred in the middle of the glacier while the front experienced slight thinning. These results imply that this surge was long-lived, possibly with multiple events, over the course of 5–10 years following the initial event in 2001. Both Doktorbreen [Dk] and Liestølbreen [L] show similar thinning between 1990 and 2003 though between 2003 to 2008 thinning increased on Doktorbreen and decreased on Listølbreen. Additionally, a region of increases around 350 m a.s.l. on Doktorbreen resemble a dynamic mass movement event. This may or may not be a precursor to a full-blown surge (Sund et al., 2009)

Full glacier volume and mass changes for both periods are not computed here for a variety of reasons. First, the time between DEMs is relatively short for the expected rates of change on the archipelago, such that volume change estimates may be quite susceptible to the various biases within the satellite DEMs. Additionally, there is a lack of data in the 1990 images (missing strip) and in the majority of the upper glacier zones within both the ASTER and SPOT5 DEMs. Recent volume and mass change numbers for this region are given in Nuth et al. (2010); Moholdt et al. (2010b).

## 7 Conclusions and perspectives

The aims of this study were to detect, analyze and statistically correct the various errors and biases that exist within publicly available elevation products. We present a simple and robust co-registration method for DEM pairs using the elevation difference residuals and the elevation derivatives of slope and aspect. This method is advantageous because it only requires 2–3 iterations as opposed to the method of RMSE minimization by iteratively shifting that requires often more than 20 iterations. The method represents the complete analytical solution of a 3-dimensional shift vector between two DEMs. The solution to Eq. (3) returns statistically significant results for situations when full continuous surface residuals are available but also when stable terrain is limited

### Correcting elevation data for glacier change detection

C. Nuth and A. Kääb

Title Page

Abstract

Introduction

Conclusions

References

Tables

Figures



Back

Close

Full Screen / Esc

Printer-friendly Version

Interactive Discussion



## Correcting elevation data for glacier change detection

C. Nuth and A. Kääb

Title Page

Abstract

Introduction

Conclusions

References

Tables

Figures

◀

▶

◀

▶

Back

Close

Full Screen / Esc

Printer-friendly Version

Interactive Discussion



to less than 10% of the scene and in comparisons between a DEM and the spatially limited ICESat elevation tracks. By triangulating the co-registration residuals between three elevation data sets, we estimate an internal precision of at least  $1/3$  but up to  $1/10$  of an ASTER or SPOT5 pixel in the horizontal and between 1–4 m vertically. The co-registration accuracy decreases with availability of stable terrain. In this study,  $\approx 600$  difference points between ICESat and ASTER effectively co-registered the data products to at least  $1/3$  of a pixel. The improvement of the standard deviation of elevation residuals through co-registration amounted 5–70% depending upon the magnitude of the shift vector. We suggest that co-registration be tested and, if necessary, performed whenever elevation differencing is used for estimation of glacier changes. The magnitude of the bias induced by not co-registering is directly related to the direction and magnitude of the shift with the direction and slope of the glacier surface. That implies that for very flat glaciers a correction effect might be small, but also that the correction effect for steeper glaciers might by far exceed the signal intended to detect. Unless there is a perfectly random distribution of (glacier) slopes and aspects within a study area, omitting to correct a significant shift will not only result in an increased RMSE of the elevation differences, but induce a systematic vertical bias.

In this study, large elevation dependent biases occurred within the ASTER DEMs that covered less than 70% of the land surface. This may imply that the spatial and elevational distribution of automatically generated tie points affects the tuning of the stereo model within the automated process. It is difficult to determine whether the SRTM has a significant elevation dependent bias; all tests were not as convincing as Fig. 3. An elevation dependent bias caused by penetration of the SRTM C band radar is however much more dangerous. Determination of this type of bias is out of the scope of this paper. More research should certainly be focused on for example, comparing glacier DEMs created at roughly the same time as the SRTM to analyze the magnitude of this bias.

Significant along/cross track biases are specifically found within the ASTER DEMs. These biases are as large as  $\pm 10$  m which we adjust using 6–8th-order polynomials. A

higher frequency bias has been detected in the automatically generated ASTER DEMs with  $\approx 10$ – $12$  cycles per scene which may be related to the under-sampled pitch of the backward looking sensor, similar to those found with the nadir looking camera (Leprince et al., 2007). The amplitude of this bias in 2–4 m, which we regard as under the significant limitation of our statistical adjustments. It is important to note, that, since every ASTER SilcAst DEM individually is infected by these high-frequency variations, a differential DEM might contain in the best case a destructive superposition of these variations (i.e. error elimination), or in the worst case a constructive superposition (i.e. error maximization). A prime example is the ASTER GDEM (Fig. 5) where constructive superposition of this variation is apparent in the lower center of the scene (in flat terrain). The longer frequency distortion however is common in all the individual ASTER DEMs we analyze both in New Zealand and in Svalbard. The cause behind this bias is uncertain to us. However, Leprince et al. (2007) who also found *jitter* did not observe the lower frequency bias. In contrast to our data (i.e. LPDAAC), they use their own sensor model involving GCPs.

The detection of glacier elevation changes using the readily available global elevation products tested in this study is dependent upon the time between measurements and the magnitude of glacier changes. In New Zealand, a single year elevation difference from satellite elevation products was clearly detected on Fox glacier. However, the 6 year changes contain the highest significance, are smoother due to reduction of the random noise (increase in the signal to noise ratio), and are less susceptible to the 1–4 m elevation bias uncertainty. This is clearly evident on the Tasman and Murchison glaciers where changes not larger than  $\approx 4$  m per year are observed. In Svalbard, changes are even smaller than New Zealand except for occasional surges. Single year detection of a surging glacier should be possible using satellite products as long as the bias can be detected and adjusted.

Estimating volume changes and associated geodetic mass balances are also affected significantly by both vertical bias as well as an elevation dependent bias. The effect of these bias on estimations of volume change is dependent upon the magnitude

## Correcting elevation data for glacier change detection

C. Nuth and A. Kääb

Title Page

Abstract

Introduction

Conclusions

References

Tables

Figures

◀

▶

◀

▶

Back

Close

Full Screen / Esc

Printer-friendly Version

Interactive Discussion



and sign of the bias in relation to the glacier hypsometry. We suggest that error may be more appropriately estimated using a hypsometric approach that includes systematic bias if known to exist. Increasing the time between DEMs improves annual average geodetic balance estimates significantly by reducing the impact of persistent bias.

As a main conclusion from our study, we suggest a methodological approach (Fig. 14) for whenever DEM (or elevation) comparison is to be performed for glacier research. The first and most important step is to test and, possibly, correct for shifts between DEMs. Our method for that can easily be implemented in free or standard geoinformation systems, table processing softwares, or standard programming environments such as MATLAB or IDL. The only functionalities necessary are: computation of DEM differences, DEM slope and aspect; simple DEM attribute algebra (here  $dh / \tan(\alpha)$ ); curve-fitting including fitting of sines or cosines; and DEM shifting. If no curve fitting functionality is available, the necessary shift parameters can straight-forward be estimated from a scatter plot as shown in Fig. 2. The method can be fully automated. The correction of any further, secondary, biases is dependent on the individual sensor systems and DEM post-processing procedures. However, it should be noted that these biases can easily mimic real glaciological processes such as surges or mass-balance variations with altitude.

We found the ICESat-derived elevations to be the most consistent globally available elevation data set available so far. It could be used as reference to register DEMs to in any regional-scale study. This would lead to a consistent global reference frame for glacier elevation change studies. As a consequence, we recommend for instance, to consider within a new compilation of the ASTER GDEM to reference any individual ASTER DEM to ICESat elevations before merging these individual DEMs to the global data set. A similar procedure, at least for testing, might be appropriate for other ongoing or future global DEM projects such as TanDEM-X or SPOT5-HRS.

*Acknowledgements.* The authors would like to thank Geir Moholdt for proofing and critically analyzing an earlier version of the manuscript. Jack Kohler, Jon Ove Hagen, and Thomas Vikhamar Schuler for always providing positive feedback and guidance. This study

## Correcting elevation data for glacier change detection

C. Nuth and A. Kääb

Title Page

Abstract

Introduction

Conclusions

References

Tables

Figures



Back

Close

Full Screen / Esc

Printer-friendly Version

Interactive Discussion



is the result of the IPY-Glaciodyn project (176076) funded by the Norwegian Research Council (NFR) and is a contribution to the ESA DUE GlobGlacier project and the ESA Climate Change Initiative (Essential Climate Variable CCI ECV “glaciers and ice caps”), which partially funded the work. The ASTER individual DEMs were provided within the framework of the Global Land Ice Measurements from Space project (GLIMS) through the USGS LPDAAC and is courtesy of NASA/GSFC/METI/ERSDAC/JAROS and the US/Japan ASTER science team. ASTER GDEM is a product of METI and NASA downloaded freely from the LPDAAC. The ICESat GLAS data were obtained from the NSIDC, Boulder. The SPOT5-HRS DEM (ID: SPI08-025-Svalbard) was obtained through the IPY-SPIRIT program (Korona et al., 2009) ©CNES 2008 and SPOT Image 2008 all rights reserved. The SRTM DEM was provided by EROS data center at the US Geological Survey. The NPI DEM and masks were provided in collaboration with the Norwegian Polar Institute.

*Author Contributions.* C.N. developed all algorithms, did all analyses and data interpretations, created the figures, and wrote the paper. A.K. contributed to the concepts, wrote and edited the paper and assisted in interpretations.

## References

- Anderson, B., Lawson, W., Owens, I., and Goodsell, B.: Past and future mass balance of ‘Ka Roimata o Hine Hukatere’ Franz Josef Glacier, New Zealand, *J. Glaciol.*, 52, 597–607, <http://dx.doi.org/10.3189/172756506781828449>, 2006. 2037, 2038
- Arendt, A. A., Echelmeyer, K. A., Harrison, W. D., Lingle, C. S., and Valentine, V. B.: Rapid wastage of Alaska glaciers and their contribution to rising sea level, *Science*, 297, 382–386, <http://dx.doi.org/10.1126/science.1072497>, 2002. 2029
- Bader, H.: Sorge’s Law of densification of snow on high polar glaciers, *J. Glaciol.*, 2, 319–323, 1954. 2030
- Berthier, E.: Volume loss from Bering Glacier, Alaska, 1972–2003: comment on Muskett and others (2009), *J. Glaciol.*, 56, 558–559, <http://dx.doi.org/10.3189/002214310792447716>, 2010. 2016
- Berthier, E. and Toutin, T.: SPOT5-HRS digital elevation models and the monitoring of glacier elevation changes in North-West Canada and South-East Alaska, *Rem. Sens. Environ.*, 112, 2443–2454, <http://dx.doi.org/10.1016/j.rse.2007.11.004>, 2008. 2019, 2020, 2022

## Correcting elevation data for glacier change detection

C. Nuth and A. Kääb

Title Page

Abstract

Introduction

Conclusions

References

Tables

Figures



Back

Close

Full Screen / Esc

Printer-friendly Version

Interactive Discussion



## Correcting elevation data for glacier change detection

C. Nuth and A. Kääb

Title Page

Abstract

Introduction

Conclusions

References

Tables

Figures

◀

▶

◀

▶

Back

Close

Full Screen / Esc

Printer-friendly Version

Interactive Discussion



- Berthier, E., Arnaud, Y., Baratoux, D., Vincent, C., and Rémy, F.: Recent rapid thinning of the “Mer de Glace” glacier derived from satellite optical images, *Geophys. Res. Lett.*, 31, L17401, doi:10.1029/2004GL020706, <http://dx.doi.org/10.1029/2004GL020706>, 2004. 2017, 2020, 2025, 2029
- 5 Berthier, E., Arnaud, Y., Vincent, C., and Rémy, F.: Biases of SRTM in high-mountain areas: Implications for the monitoring of glacier volume changes, *Geophys. Res. Lett.*, 33, L08502, <http://dx.doi.org/10.1029/2006GL025862>, 2006. 2020, 2025, 2026, 2040
- Berthier, E., Arnaud, Y., Kumar, R., Ahmad, S., Wagnon, P., and Chevallier, P.: Remote sensing estimates of glacier mass balances in the Himachal Pradesh (Western Himalaya, India), *Rem. Sens. Environ.*, 108, 327–338, <http://dx.doi.org/10.1016/j.rse.2006.11.017>, 2007.
- 10 2016, 2017, 2020, 2022, 2025, 2026
- Berthier, E., Schiefer, E., Clarke, G. K. C., Menounos, B., and Remy, F.: Contribution of Alaskan glaciers to sea-level rise derived from satellite imagery, *Nature Geosci.*, 3, 92–95, <http://dx.doi.org/10.1038/ngeo737>, 2010. 2016, 2017, 2025, 2028, 2029
- 15 Bolch, T., Buchroithner, M., Pieczonka, T., and Kunert, A.: Planimetric and volumetric glacier changes in the Khumbu Himal, Nepal, since 1962 using Corona, Landsat TM and ASTER data, *J. Glaciol.*, 54, 592–600, <http://dx.doi.org/10.3189/002214308786570782>, 2008. 2016
- Bouillon, A., Bernard, M., Gigord, P., Orsoni, A., Rudowski, V., and Baudoin, A.: SPOT 5 HRS geometric performances: Using block adjustment as a key issue to improve quality of DEM generation, *ISPRS Journal of Photogrammetry and Remote Sensing*, 60, 134–146, <http://dx.doi.org/10.1016/j.isprsjprs.2006.03.002>, 2006. 2019, 2020
- 20 20 Brenner, A. C., DiMarzio, J. R., and Zwally, H. J.: Precision and accuracy of satellite radar and laser altimeter data over the continental ice sheets, *IEEE Transactions on Geoscience and Remote Sensing*, 45, 321–331, <http://dx.doi.org/10.1109/TGRS.2006.887172>, 2007. 2021, 2041
- 25 Bretherton, C. S., Widmann, M., Dymnikov, V. P., Wallace, J. M., and Blad, I.: The Effective Number of Spatial Degrees of Freedom of a Time-Varying Field, *J. Climate*, 12, 1990–2009, [http://dx.doi.org/10.1175/1520-0442\(1999\)012<1990:TENOSD>2.0.CO;2](http://dx.doi.org/10.1175/1520-0442(1999)012<1990:TENOSD>2.0.CO;2), 1999. 2028
- Burrough, P., McDonnell, R., and Burrough, P.: Principles of geographical information systems, Oxford University Press, Oxford, 1998. 2028
- 30 Davis, J. C.: Statistics and data analysis in geology, J. Wiley, New York, 2002. 2028
- Dowdeswell, J. A. and Benham, T. J.: A surge of Perseibreen, Svalbard, examined using aerial photography and ASTER high resolution satellite imagery, *Polar Research*, 22, 373–383,

## Correcting elevation data for glacier change detection

C. Nuth and A. Kääb

Title Page

Abstract

Introduction

Conclusions

References

Tables

Figures

◀

▶

◀

▶

Back

Close

Full Screen / Esc

Printer-friendly Version

Interactive Discussion



<http://dx.doi.org/10.1111/j.1751-8369.2003.tb00118.x>, 2003. 2044

Elsberg, D. H., Harrison, W. D., Echelmeyer, K. A., and Krimmel, R. M.: Quantifying the effects of climate and surface change on glacier mass balance, *J. Glaciol.*, 47, 649–658, <http://dx.doi.org/10.3189/172756501781831783>, 2001. 2029

5 ERSDAC: ASTER Users Guide Part III. DEM Product (L4A01). (Ver.1.1), Tech. rep., Earth Remote Sensing Data Analysis Center (ERSDAC), [http://www.science.aster.ersdac.or.jp/en/documnts/users\\_guide/index.html](http://www.science.aster.ersdac.or.jp/en/documnts/users_guide/index.html), 2005. 2019

ERSDAC: ASTER Users Guide Part II Level 1 Data Products (Ver.5.1), Tech. rep., Earth Remote Sensing Data Analysis Center (ERSDAC), [http://www.science.aster.ersdac.or.jp/en/documnts/users\\_guide/index.html](http://www.science.aster.ersdac.or.jp/en/documnts/users_guide/index.html), 2007. 2026, 2035

10 Etzelmüller, B.: On the Quantification of Surface Changes using Grid-based Digital Elevation Models (DEMs), *Transactions in GIS*, 4, 129–143, <http://dx.doi.org/10.1111/1467-9671.00043>, 2000. 2028, 2029

15 Farr, T. G., Rosen, P. A., Caro, E., Crippen, R., Duren, R., Hensley, S., Kobrick, M., Paller, M., Rodriguez, E., Roth, L., Seal, D., Shaffer, S., Shimada, J., Umland, J., Werner, M., Oskin, M., Burbank, D., and Alsdorf, D.: The Shuttle Radar Topography Mission, *Rev. Geophys.*, 45, RG2004, <http://dx.doi.org/10.1029/2005RG000183>, 2007. 2015, 2020, 2027

Finsterwalder, R.: Photogrammetry and glacier research with special reference to glacier retreat in the eastern Alps, *J. Glaciol.*, 2, 306–314, 1954. 2016

20 Fisher, P.: Improved Modeling of Elevation Error with Geostatistics, *Geoinformatica*, 2, 215–233, <http://dx.doi.org/10.1023/A:1009717704255>, 1998. 2027

Fitzharris, B., Lawson, W., and Owens, I.: Research on glaciers and snow in New Zealand, *Progress In Physical Geography*, 23, 469–500, <http://dx.doi.org/10.1177/030913339902300402>, 1999. 2037

25 Fricker, H. A., Borsa, A., Minster, B., Carabajal, C., Quinn, K., and Bills, B.: Assessment of ICESat performance at the Salar de Uyuni, Bolivia, *Geophys. Res. Lett.*, 32, 5, <http://dx.doi.org/10.1029/2005GL023423>, 2005. 2021, 2041

Fujisada, H., Bailey, G., Kelly, G., Hara, S., and Abrams, M.: ASTER DEM performance, *Geosci. Rem. Sens., IEEE Transactions*, 43, 2707–2714, <http://dx.doi.org/10.1109/TGRS.2005.847924>, 2005. 2019, 2020

30 GADM: GADM database of Global Administrative Areas, <http://www.gadm.org> [Online-Accessed 21.Sept.2010], 2010. 2023

Gjermundsen, E. F.: Recent changes in glacier area in the Central Southern Alps of New

**Correcting elevation data for glacier change detection**

C. Nuth and A. Kääb

Title Page

Abstract

Introduction

Conclusions

References

Tables

Figures

◀

▶

◀

▶

Back

Close

Full Screen / Esc

Printer-friendly Version

Interactive Discussion



Zealand, Master's thesis, University of Oslo, 2007. 2023

Gorokhovich, Y. and Voustianiouk, A.: Accuracy assessment of the processed SRTM-based elevation data by CGIAR using field data from USA and Thailand and its relation to the terrain characteristics, *Remote Sensing of Environment*, 104, 409–415, <http://dx.doi.org/10.1016/j.rse.2006.05.012>, 2006. 2016, 2022, 2023

Gruen, A. and Akca, D.: Least squares 3D surface and curve matching, *Isprs Journal of Photogrammetry and Remote Sensing*, 59, 151–174, <http://dx.doi.org/10.1016/j.isprsjprs.2005.02.006>, 2005. 2017, 2022

Hagg, W. J., Braun, L. N., Uvarov, V. N., and Makarevich, K. G.: A comparison of three methods of mass-balance determination in the Tuyuksu glacier region, Tien Shan, Central Asia, *J. Glaciol.*, 50, 505–510, <http://dx.doi.org/10.3189/172756504781829783>, 2004. 2030

Hirano, A., Welch, R., and Lang, H.: Mapping from ASTER stereo image data: DEM validation and accuracy assessment, *Isprs Journal of Photogrammetry and Remote Sensing*, 57, 356–370, [http://dx.doi.org/10.1016/S0924-2716\(02\)00164-8](http://dx.doi.org/10.1016/S0924-2716(02)00164-8), 2003. 2020

Hisdal, V.: *Geography of Svalbard*, vol. 2, Norwegian Polar Institute, Oslo, 1985. 2040

Hochstein, M. P., Claridge, D., Henrys, S. A., Pyne, A., Nobes, D. C., and Leary, S. F.: Drowning of the Tasman Glacier, South Island, New-zealand – Changes In the Terminus Region Between 1971 and 1993, *New Zealand Journal of Geology and Geophysics*, 38, 1–16, <http://dx.doi.org/10.1080/00288306.1995.9514635>, 1995. 2038

Howat, I. M., Smith, B. E., Joughin, I., and Scambos, T. A.: Rates of southeast Greenland ice volume loss from combined ICESat and ASTER observations, *Geophys. Res. Lett.*, 35, L17505, doi:10.1029/2008GL034496, <http://dx.doi.org/10.1029/2008GL034496>, 2008. 2016, 2021, 2022

Iwasaki, A. and Fujisada, H.: ASTER geometric performance, *Geoscience and Remote Sensing*, *IEEE Transactions on DOI – 10.1109/TGRS.2005.849055*, 43, 2700–2706, 10.1109/TGRS.2005.849055, 2005. 2020

Kääb, A.: *Remote Sensing of Mountain Glaciers and Permafrost Creep*, Geographisches Institut der Universität Zürich, Zürich, 2005. 2019, 2020, 2023, 2024

Kääb, A.: Glacier Volume Changes Using ASTER Satellite Stereo and ICESat GLAS Laser Altimetry. A Test Study on Edgeya, Eastern Svalbard, *IEEE International Geoscience and Remote Sensing*, 46, 2823–2830, <http://dx.doi.org/10.1109/TGRS.2008.2000627>, 2008. 2017, 2021, 2025, 2028, 2029

Kääb, A., Huggel, C., Paul, F., Wessels, R., Raup, B., Kieffer, H., and Kargel, J.: *Glacier*

---

**Correcting elevation data for glacier change detection**C. Nuth and A. Kääb

---

[Title Page](#)[Abstract](#)[Introduction](#)[Conclusions](#)[References](#)[Tables](#)[Figures](#)[Back](#)[Close](#)[Full Screen / Esc](#)[Printer-friendly Version](#)[Interactive Discussion](#)

- monitoring from ASTER imagery: Accuracy and Applications, in: Proceedings of EARSeL-LISSIG-Workshop Observing our Cryosphere from Space, 2002. 2020
- Kirkbride, M. P.: Relationships Between Temperature and Ablation On the Tasman Glacier, Mount Cook National-park, New-zealand, New Zealand Journal of Geology and Geophysics, 38, 17–27, <http://dx.doi.org/10.1080/00288306.1995.9514636>, 1995. 2037
- Knöpfle, W., Strunz, G., and Roth, A.: Mosaicking of Digital Elevation Models derived by SAR interferometry, ISPRS Commission IV Symposium on GIS – Between Visions and Applications, 32, 1998. 2027
- Kohler, J., James, T. D., Murray, T., Nuth, C., Brandt, O., Barrand, N. E., Aas, H. F., and Luckman, A.: Acceleration in thinning rate on western Svalbard glaciers, Geophysical Research Letters, 34, 5, <http://dx.doi.org/10.1029/2007GL030681>, 2007. 2029
- König, M., Winther, J. G., and Isaksson, E.: Measuring snow and glacier ice properties from satellite, Rev. Geophys., 39, 1–27, <http://dx.doi.org/10.1029/1999RG000076>, 2001. 2036
- Korona, J., Berthier, E., Bernard, M., Rémy, F., and Thouvenot, E.: SPIRIT. SPOT 5 stereoscopic survey of Polar Ice: Reference Images and Topographies during the fourth International Polar Year (2007-2009), Isprs Journal of Photogrammetry and Remote Sensing, 64, 204–212, <http://dx.doi.org/10.1016/j.isprsjprs.2008.10.005>, 2009. 2019, 2020, 2021, 2040, 2049
- Larsen, C. F., Motyka, R. J., Arendt, A. A., Echelmeyer, K. A., and Geissler, P. E.: Glacier changes in southeast Alaska and northwest British Columbia and contribution to sea level rise, J. Geophys. Res.-Earth Surface, 112, F01007, doi:10.1029/2006JF000586, <http://dx.doi.org/10.1029/2006JF000586>, 2007. 2020
- Leprince, S., Ayoub, F., Klingert, Y., and Avouac, J.-P.: Co-Registration of Optically Sensed Images and Correlation (COSI-Corr): an operational methodology for ground deformation measurements, in: Geoscience and Remote Sensing Symposium, 2007, IGARSS 2007, IEEE International, pp. 1943–1946, doi:10.1109/IGARSS.2007.4423207, 2007. 2020, 2026, 2035, 2047
- Li, Z. L.: On the Measure of Digital Terrain Model Accuracy, Photogrammetric Record, 12, 873–877, <http://dx.doi.org/10.1111/j.1477-9730.1988.tb00636.x>, 1988. 2027
- Lillesand, T., Kiefer, R., and Chipman, J.: Remote Sensing and Image Interpretation, John Wiley & Sons, Inc., 5 edn., 2004. 2018
- Luthcke, S. B., Rowlands, D. D., Williams, T. A., and Sirota, M.: Reduction of ICESat systematic geolocation errors and the impact on ice sheet elevation change detection, Geophys. Res.

Lett., 32(4), L21S05, doi:10.1029/2005GL023689, <http://dx.doi.org/10.1029/2005GL023689>, 2005. 2041

Magruder, L., Silverberg, E., Webb, C., and Schutz, B.: In situ timing and pointing verification of the ICESat altimeter using a ground-based system, *Geophys. Res. Lett.*, 32(5), L21S04, doi:10.1029/2005GL023504, <http://dx.doi.org/10.1029/2005GL023504>, 2005. 2041

METI/NASA/USGS: ASTER Global DEM Validation Summary Report, Tech. rep., METI/ERSDAC, NASA/LPDAAC, USGS/EROS, 2009. 2015, 2021, 2031

Mikhail, E., Bethel, J., and McGlone, J. C.: *Introduction to Modern Photogrammetry*, John Wiley & Sons, Inc., 2001. 2018

Miller, P. E., Kunz, M., Mills, J. P., King, M. A., Murray, T., James, T. D., and Marsh, S. H.: Assessment of Glacier Volume Change Using ASTER-Based Surface Matching of Historical Photography, *IEEE Transactions On Geoscience and Remote Sensing*, 47, 1971–1979, <http://dx.doi.org/10.1109/TGRS.2009.2012702>, 2009. 2022

Moholdt, G., Hagen, J. O., Eiken, T., and Schuler, T. V.: Geometric changes and mass balance of the Austfonna ice cap, Svalbard, *The Cryosphere*, 4, 21–34, doi:10.5194/tc-4-21-2010, 2010a. 2021

Moholdt, G., Nuth, C., Hagen, J. O., and Kohler, J.: Recent elevation changes of Svalbard glaciers derived from ICESat laser altimetry, *Rem. Sens. Environ.*, 114, 2756–2767, <http://dx.doi.org/10.1016/j.rse.2010.06.008>, 2010b. 2021, 2030, 2032, 2043, 2045

Müller, K., Hamran, S.-E., Sinisalo, A., and Hagen, J.-O.: Microwave backscatter from Arctic firn and its relation to the phase center, *IEEE Transactions On Geoscience and Remote Sensing*, submitted, 2010. 2037

Muskett, R. R., Lingle, C. S., Sauber, J. M., Post, A. S., Tangborn, W. V., Rabus, B. T., and Echelmeyer, K. A.: Airborne and spaceborne DEM- and laser altimetry-derived surface elevation and volume changes of the Bering Glacier system, Alaska, USA, and Yukon, Canada, 1972–2006, *J. Glaciol.*, 55, 316–326, <http://dx.doi.org/10.3189/002214309788608750>, 2009. 2016

NASA, NGA, DLR, and ASI: Shuttle Radar Topography Mission (SRTM) Elevation Data Set, <http://seamless.usgs.gov>, 2002. 2020

Nuth, C., Kohler, J., Aas, H. F., Brandt, O., and Hagen, J. O.: Glacier geometry and elevation changes on Svalbard (1936–90): a baseline dataset, *Ann. Glaciol.*, 46, 106–116, <http://dx.doi.org/10.3189/172756407782871440>, 2007. 2028, 2041

Nuth, C., Moholdt, G., Kohler, J., Hagen, J. O., and Kääb, A.: Svalbard glacier eleva-

TCD

4, 2013–2077, 2010

## Correcting elevation data for glacier change detection

C. Nuth and A. Kääb

Title Page

Abstract

Introduction

Conclusions

References

Tables

Figures

◀

▶

◀

▶

Back

Close

Full Screen / Esc

Printer-friendly Version

Interactive Discussion



## Correcting elevation data for glacier change detection

C. Nuth and A. Käab

Title Page

Abstract

Introduction

Conclusions

References

Tables

Figures



Back

Close

Full Screen / Esc

Printer-friendly Version

Interactive Discussion



tion changes and contribution to sea level rise, *J. Geophys. Res.*, 115, F01008, <http://dx.doi.org/10.1029/2008JF001223>, 2010. 2021, 2029, 2041, 2043, 2045

Oerlemans, J., Bassford, R. P., Chapman, W., Dowdeswell, J. A., Glazovsky, A. F., Hagen, J. O., Melvold, K., de Wildt, M. D., and van de Wal, R. S. W.: Estimating the contribution of Arctic glaciers to sea-level change in the next 100 years, *Ann. Glaciol.*, 42, 230–236, <http://dx.doi.org/10.3189/172756405781812745>, 2005. 2037

Paul, F.: Calculation of glacier elevation changes with SRTM: is there an elevation-dependent bias?, *J. Glaciol.*, 54, 945–946, <http://dx.doi.org/10.3189/002214308787779960>, 2008. 2017, 2023, 2026, 2033

Paul, F. and Haeberli, W.: Spatial variability of glacier elevation changes in the Swiss Alps obtained from two digital elevation models, *Geophys. Res. Lett.*, 35, L21502, [doi:10.1029/2008GL034718](https://doi.org/10.1029/2008GL034718), <http://dx.doi.org/10.1029/2008GL034718>, 2008. 2020, 2029

Peduzzi, P., Herold, C., and Silverio, W.: Assessing high altitude glacier thickness, volume and area changes using field, GIS and remote sensing techniques: the case of Nevado Coropuna (Peru), *The Cryosphere*, 4, 313–323, [doi:10.5194/tc-4-313-2010](https://doi.org/10.5194/tc-4-313-2010), 2010. 2016, 2022, 2023

Pritchard, H. D., Arthern, R. J., Vaughan, D. G., and Edwards, L. A.: Extensive dynamic thinning on the margins of the Greenland and Antarctic ice sheets, *Nature*, 461, 971–975, <http://dx.doi.org/10.1038/nature08471>, 2009. 2021

Purdie, H. L., Brook, M. S., and Fuller, I. C.: Seasonal variation in ablation and surface velocity on a temperate maritime Glacier: Fox Glacier, New Zealand, *Arctic Antarctic and Alpine Research*, 40, 140–147, [http://dx.doi.org/10.1657/1523-0430\(06-032\)\[PURDIE\]2.0.CO;2](http://dx.doi.org/10.1657/1523-0430(06-032)[PURDIE]2.0.CO;2), 2008. 2038

Quincey, D. J. and Glasser, N. F.: Morphological and ice-dynamical changes on the Tasman Glacier, New Zealand, 1990-2007, *Global and Planetary Change*, 68, 185–197, <http://dx.doi.org/10.1016/j.gloplacha.2009.05.003>, 2009. 2038

Rabus, B., Eineder, M., Roth, A., and Bamler, R.: The shuttle radar topography mission – a new class of digital elevation models acquired by spaceborne radar, *ISPRS Journal of Photogrammetry and Remote Sensing*, 57, 241–262, [http://dx.doi.org/10.1016/S0924-2716\(02\)00124-7](http://dx.doi.org/10.1016/S0924-2716(02)00124-7), 2003. 2020, 2021

Racoviteanu, A. E., Manley, W. F., Arnaud, Y., and Williams, M. W.: Evaluating digital elevation models for glaciologic applications: An example from Nevado Coropuna, Peruvian Andes, *Global and Planetary Change*, 59, 110–125, <http://dx.doi.org/10.1016/j.gloplacha.2006.11.036>, 2007. 2016, 2022

- Rignot, E., Echelmeyer, K., and Krabill, W.: Penetration depth of interferometric synthetic-aperture radar signals in snow and ice, *Geophys. Res. Lett.*, 28, 3501–3504, <http://dx.doi.org/10.1029/2000GL012484>, 2001. 2020, 2026, 2036
- Rignot, E., Rivera, A., and Casassa, G.: Contribution of the Patagonia Icefields of South America to sea level rise, *Science*, 302, 434–437, <http://dx.doi.org/10.1126/science.1087393>, 2003. 2016, 2020
- Rodriguez, E., Morris, C. S., and Belz, J. E.: A global assessment of the SRTM performance, *Photogrammetric Engineering and Remote Sensing*, 72, 249–260, 2006. 2016, 2020
- Rolstad, C., Haug, T., and Denby, B.: Spatially integrated geodetic glacier mass balance and its uncertainty based on geostatistical analysis: application to the western Svartisen ice cap, Norway, *J. Glaciol.*, 55, 666–680, <http://dx.doi.org/10.3189/002214309789470950>, 2009. 2028
- Rosen, P. A., Hensley, S., Joughin, I. R., Li, F. K., Madsen, S. N., Rodriguez, E., and Goldstein, R. M.: Synthetic aperture radar interferometry, Invited paper, *Proceedings of the IEEE*, 88, 333–382, <http://dx.doi.org/10.1109/5.838084>, 2000. 2020
- Sapiano, J., Harrison, W., and Echelmeyer, K.: Elevation, volume and terminus changes of nine glaciers in North America, *J. Glaciol.*, 44, 119–135, 1998. 2030
- Schenk, T.: *Digital Photogrammetry*, vol. 1, TerraScience, 1999. 2019
- Schenk, T., Csatho, B., van der Veen, C. J., Brecher, H., Ahn, Y., and Yoon, T.: Registering imagery to ICESat data for measuring elevation changes on Byrd Glacier, Antarctica, *Geophys. Res. Lett.*, 32(4), L23S05, doi:10.1029/2005GL024328, <http://dx.doi.org/10.1029/2005GL024328>, 2005. 2042
- Schiefer, E., Menounos, B., and Wheate, R.: Recent volume loss of British Columbian glaciers, Canada, *Geophys. Res. Lett.*, 34, L16503, doi:10.1029/2007GL030780, <http://dx.doi.org/10.1029/2007GL030780>, 2007. 2020, 2023, 2026
- Skinner, B.: Measurement of twentieth century ice loss on the Tasman Glacier, New Zealand, *New Zealand Journal of Geology and Geophysics*, 7, 796–803, 1964. 2038
- Sund, M., Eiken, T., Hagen, J. O., and Kääb, A.: Svalbard surge dynamics derived from geometric changes, *Ann. Glaciol.*, 50, doi:10.3189/172756409789624265, <http://dx.doi.org/10.3189/172756409789624265>, 2009. 2016, 2038, 2044, 2045
- Surazakov, A. B. and Aizen, V. B.: Estimating volume change of mountain glaciers using SRTM and map-based topographic data, *IEEE Transactions on Geoscience and Remote Sensing*, 44, 2991–2995, <http://dx.doi.org/10.1109/TGRS.2006.875357>, 2006. 2026

## Correcting elevation data for glacier change detection

C. Nuth and A. Kääb

Title Page

Abstract

Introduction

Conclusions

References

Tables

Figures

◀

▶

◀

▶

Back

Close

Full Screen / Esc

Printer-friendly Version

Interactive Discussion



**Correcting elevation data for glacier change detection**

C. Nuth and A. Kääb

Title Page

Abstract

Introduction

Conclusions

References

Tables

Figures

◀

▶

◀

▶

Back

Close

Full Screen / Esc

Printer-friendly Version

Interactive Discussion



Toutin, T.: Three-dimensional topographic mapping with ASTER stereo data in rugged topography, *IEEE Transactions on Geoscience and Remote Sensing*, 40, 2241–2247, <http://dx.doi.org/10.1109/TGRS.2002.802878>, 2002. 2020

5 Toutin, T.: Review article: Geometric processing of remote sensing images: models, algorithms and methods, *Int. J. Rem. Sens.*, 25, 1893–1924, <http://dx.doi.org/10.1080/0143116031000101611>, 2004. 2019

Toutin, T.: ASTER DEMs for geomatic and geoscientific applications: a review, *Int. J. Rem. Sens.*, 29, 1855–1875, <http://dx.doi.org/10.1080/01431160701408477>, 2008. 2018, 2019, 2020

10 WGMS: Fluctuations of Glaciers 20002005, vol. IX, ICSU(FAGS)/IUGG(IACS)/UNEP/UNESCO/WMO, World Glacier Monitoring Service, Zurich, Switzerland., 2008. 2038, 2039

Wilson, J. and Gallant, J.: *Terrain Analysis. Principles and Applications*, John Wiley & Sons, Inc., 2000. 2024

15 Zwally, H., Schutz, R., Bentley, C., Bufton, J., Herring, T., Minster, J., Spinhirne, J., and Thomas., R.: GLAS/ICESat L2 Global ElevationData V031, February 2003 to November 2009, 2010a. 2021

Zwally, H., Schutz, R., Bentley, C., Bufton, J., Herring, T., Minster, J., Spinhirne, J., and Thomas., R.: GLAS/ICESat L2 Global Land Surface Altimetry Data V531, February 2003 to November 2009, 2010b. 2021

20 Zwally, H. J., Schutz, B., Abdalati, W., Abshire, J., Bentley, C., Brenner, A., Bufton, J., Dezio, J., Hancock, D., Harding, D., Herring, T., Minster, B., Quinn, K., Palm, S., Spinhirne, J., and Thomas, R.: ICESat's laser measurements of polar ice, atmosphere, ocean, and land, *J. Geodynamics*, 34, 405–445, [http://dx.doi.org/10.1016/S0264-3707\(02\)00042-X](http://dx.doi.org/10.1016/S0264-3707(02)00042-X), 2002. 2015, 2021

## Correcting elevation data for glacier change detection

C. Nuth and A. Kääb

**Table 1.** New Zealand elevation data type, date acquisition, resolution, and scene id.

Data type	Date	Res. (m)	Scene ID
SRTM	11–22 Feb 2000	90	–
ASTER	7 Apr 2001	30	L1A.003:2007486672
ASTER	14 Feb 2002	30	L1A.003:2013763401
ASTER	24 Feb 2003	30	L1A.003:2011883607
ASTER	9 Feb 2006	30	L1A.003:2033045873

Title Page

Abstract

Introduction

Conclusions

References

Tables

Figures



Back

Close

Full Screen / Esc

Printer-friendly Version

Interactive Discussion



## Correcting elevation data for glacier change detection

C. Nuth and A. Kääb

**Table 2.** New Zealand southern Alps. ASTER DEM and SRTM difference statistics on stable terrain ( $\sigma$ ) for the original population of elevation differences after adjusting for the mean and for each correction applied, in sequence. The parameter solutions for the corrections are given for both the shifting correction and the elevation bias correction. The improvement of the standard deviation is the total improvement of all three corrections. The units for all parameters are meters except for  $\kappa$  which has the units meters per 1000 m.

Difference	Original	Corr. 1 – Shifting				Corr. 2 – Elevation bias			Corr. 3 – Along/cross track		Improvement in $\sigma$ (%)
	$\sigma$	$a$	$b$	$\overline{dh}$	$\sigma$	$\kappa$	$\tau$	$\sigma$	Type	$\sigma$	
2000–2001	17.0	12	58	–23	16.3	6.6	–1.3	15.2	Along	13.8	19
2000–2002	12.5	14	215	–3	11.1	0.9	–1.4	11.0	Along/cross	10.3	18
2000–2003	14.5	7	341	2	13.9	10.1	–6.8	12.1	Along	11.3	22
2000–2006	17.8	31	38	4	11.4	3.3	–4.7	11.3	Along/cross	10.6	40
2001–2002	23.9	29	205	24	17.9	–4.3	5.5	17.6	Along/cross	16.4	31
2001–2003	17.3	12	270	26	16.4	5.1	–5.8	16.4	Along	15.9	8
2001–2006	18.5	14	62	30	16.6	–3.1	3.1	16.3	Along	14.7	21
2002–2003	20.4	27	5	1	14.1	10.3	–11.7	12.0	Along/cross	12.0	41
2002–2006	24.9	46	34	7	8.0	1.2	–1.8	8.0	Along	7.7	69
2003–2006	19.4	26	70	5	13.9	–9.0	9.0	12.0	Along/cross	11.1	43

[Title Page](#)
[Abstract](#)
[Introduction](#)
[Conclusions](#)
[References](#)
[Tables](#)
[Figures](#)
[Back](#)
[Close](#)
[Full Screen / Esc](#)
[Printer-friendly Version](#)
[Interactive Discussion](#)


## Correcting elevation data for glacier change detection

C. Nuth and A. Kääb

**Table 3.** The universal shift correction vector residuals and the RSS (Root Sum of Squares) of the total vector mean and standard deviations of the elevation change residuals as solved through triangulation of three DEMs.  $\overline{dz}$  and  $\sigma_{dz}$  are the mean and standard deviation of the triple vertical difference in the DEMs. These estimates represent an internal coherency between the three datasets that reflect the residual shift that result from uncertainties in the solution of the universal co-registration correction.

Residual	$\varepsilon_x$	$\varepsilon_y$	$\varepsilon_z$	$\varepsilon_{\text{RSS}}$	$\overline{dz}$	$\sigma_{dz}$
2001-2002-2003	0.3	2.3	-0.4	2.4	-0.3	2.7
2000-2002-2006	2.4	-1.3	-0.4	2.7	-0.4	2.7
2000-2001-2003	-0.1	0.6	0.7	0.9	0.7	2.0
2001-2003-2006	2.0	-0.8	0.7	2.3	0.6	2.6
2002-2003-2006	-2.7	0.3	-1.6	3.1	-1.6	2.8
2001-2002-2006	5.0	1.1	1.9	5.5	1.8	3.9
2000-2001-2006	-10.9	4.0	2.6	11.9	3.1	6.2
2000-2003-2006	-8.7	2.5	2.6	9.5	2.9	5.2
2000-2002-2003	8.5	-3.5	-4.6	10.3	-4.9	4.9
2000-2001-2002	-8.3	6.4	4.9	11.5	5.4	5.5

[Title Page](#)
[Abstract](#)
[Introduction](#)
[Conclusions](#)
[References](#)
[Tables](#)
[Figures](#)
[Back](#)
[Close](#)
[Full Screen / Esc](#)
[Printer-friendly Version](#)
[Interactive Discussion](#)




## Correcting elevation data for glacier change detection

C. Nuth and A. Kääb

**Table 5.** Shift vectors between the 4 data types in Svalbard as tested in Case Study 2 (Sect. 6.1).  $\Delta X$ ,  $\Delta Y$  and  $\Delta Z$  are the 3 components of the full co-registration adjustment vector between the datasets in meters and the RMSE is calculated after correction.

Source	Vector	Iterations	Sample size	$\Delta X$	$\Delta Y$	$\Delta Z$	RMSE
DEM – ICESat	<b>DI</b>	2	4399	1.9	1.3	-1.0	3.6
SPOT – DEM	<b>SD</b>	3	1 173 537	-19.0	3.1	2.7	8.5
SPOT – ICESat	<b>SI</b>	3	6662	-16.8	6.3	2.5	5.1
ASTER – DEM	<b>AD</b>	3	271 784	-93.6	8.8	27.1	16.5
ASTER – SPOT	<b>AS</b>	3	289 830	-77.0	5.8	22.9	16.1
ASTER – ICESat	<b>AI</b>	2	588	-103.2	14.5	27.0	20.0

[Title Page](#)
[Abstract](#)
[Introduction](#)
[Conclusions](#)
[References](#)
[Tables](#)
[Figures](#)
[⏪](#)
[⏩](#)
[◀](#)
[▶](#)
[Back](#)
[Close](#)
[Full Screen / Esc](#)
[Printer-friendly Version](#)
[Interactive Discussion](#)


## Correcting elevation data for glacier change detection

C. Nuth and A. Kääb

Title Page

Abstract

Introduction

Conclusions

References

Tables

Figures

⏪

⏩

◀

▶

Back

Close

Full Screen / Esc

Printer-friendly Version

Interactive Discussion



**Table 6.** Error vectors revealed through triangulation. All units are meters.

Abbr	Error Vector equation	$\varepsilon_x$	$\varepsilon_y$	$\varepsilon_z$	$\varepsilon_{\text{rss}}$
SDI	<b>[SD + DI] – SI</b>	–0.3	–1.9	–0.8	2.1
ASD	<b>[AD – AS] – SD</b>	2.4	–0.2	1.4	2.8
ADI	<b>[AD + DI] – AI</b>	11.5	–4.4	–1.0	12.4
AIS	<b>[AI – SI] – AS</b>	9.8	2.4	1.6	9.85

## Correcting elevation data for glacier change detection

C. Nuth and A. Kääb

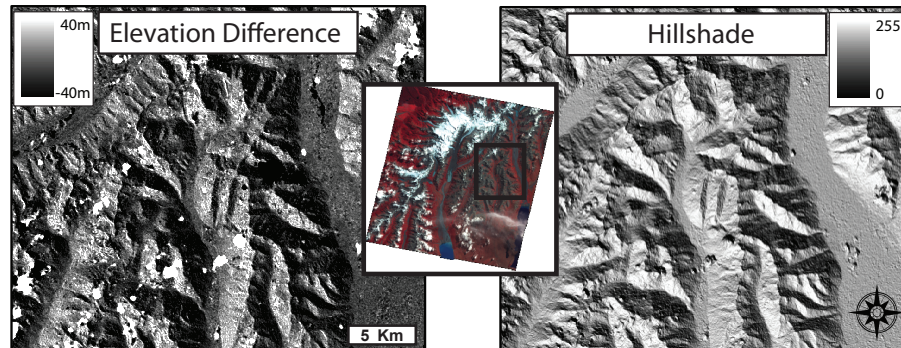


**Fig. 1.** The elevation differences before shifting (left) between ASTER DEMs in 2006 and 2002 from New Zealand (described in Sect. 5.3 and shown in Fig. 7) are remarkably similar to the hillshade of the DEMs (right). The location of the subsetting region is depicted in the 2006 ASTER image (center).

Title Page

Abstract

Introduction

Conclusions

References

Tables

Figures

◀

▶

◀

▶

Back

Close

Full Screen / Esc

Printer-friendly Version

Interactive Discussion



## Correcting elevation data for glacier change detection

C. Nuth and A. Kääb

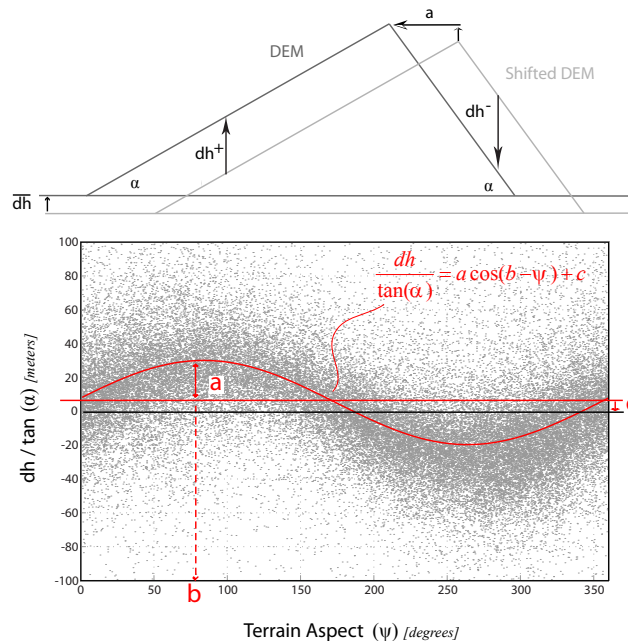


**Fig. 2.** Top: 2-dimensional scheme of elevation differences induced by a DEM shift. Bottom: The scatter of elevation differences between 2 DEMs showing the relationship between the vertical deviations normalized by the slope tangent (y-axis) and terrain aspect (x-axis). The example is the DEM differences between the 2002 and 2003 DEM used in Case Study 1 (Sect. 5). The equation for the solved sinusoidal curve fit is shown along with the three unknown solution parameters,  $a$ ,  $b$  and  $c$ .

Title Page

Abstract Introduction

Conclusions References

Tables Figures

◀ ▶

◀ ▶

Back Close

Full Screen / Esc

Printer-friendly Version

Interactive Discussion

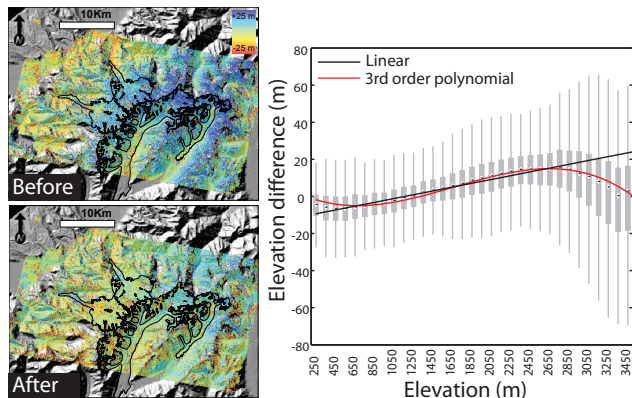


**Fig. 3.** Example of elevation differences between 2003 and 2002 ASTER DEMs from Case-Study 1 (Sect. 5.3) before and after applying an elevation dependent bias correction using a 3rd order polynomial. The two DEMs were first co-registered before checking for an elevation dependent bias. Glacier masks are indicated by black outlines.

## Correcting elevation data for glacier change detection

C. Nuth and A. Kääb

Title Page

Abstract

Introduction

Conclusions

References

Tables

Figures

◀

▶

◀

▶

Back

Close

Full Screen / Esc

Printer-friendly Version

Interactive Discussion



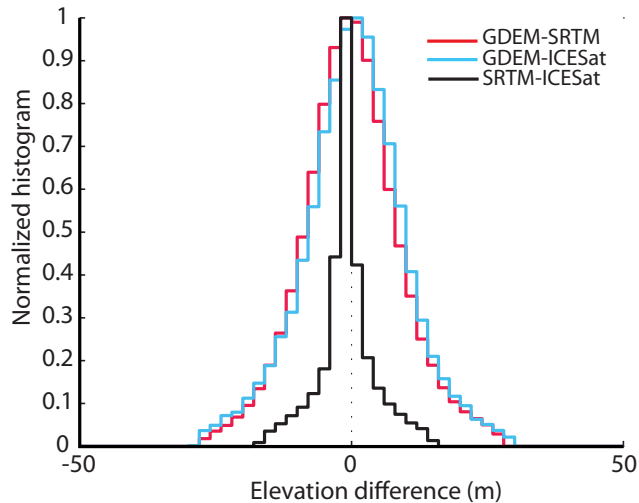


**Fig. 4.** Histograms of the stable terrain elevation differences after co-registration between the three elevation data global products tested in Case Study 1 (Sect. 5.1): the SRTM, ICESat, and the ASTER GDEM.

**Correcting elevation data for glacier change detection**

C. Nuth and A. Kääb

Title Page

Abstract Introduction

Conclusions References

Tables Figures

◀ ▶

◀ ▶

Back Close

Full Screen / Esc

Printer-friendly Version

Interactive Discussion



## Correcting elevation data for glacier change detection

C. Nuth and A. Kääb

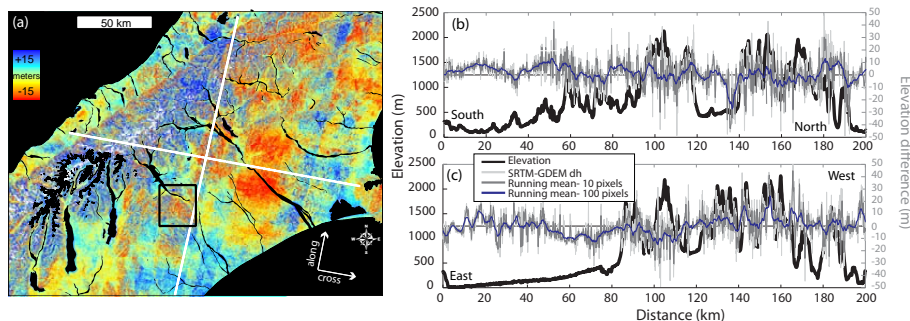


**Fig. 5.** Vertical differences between SRTM and the ASTER GDEM (a). Elevation changes exemplified for along (b) and cross track (c) profiles.

Title Page

Abstract

Introduction

Conclusions

References

Tables

Figures

◀

▶

◀

▶

Back

Close

Full Screen / Esc

Printer-friendly Version

Interactive Discussion



## Correcting elevation data for glacier change detection

C. Nuth and A. Kääb

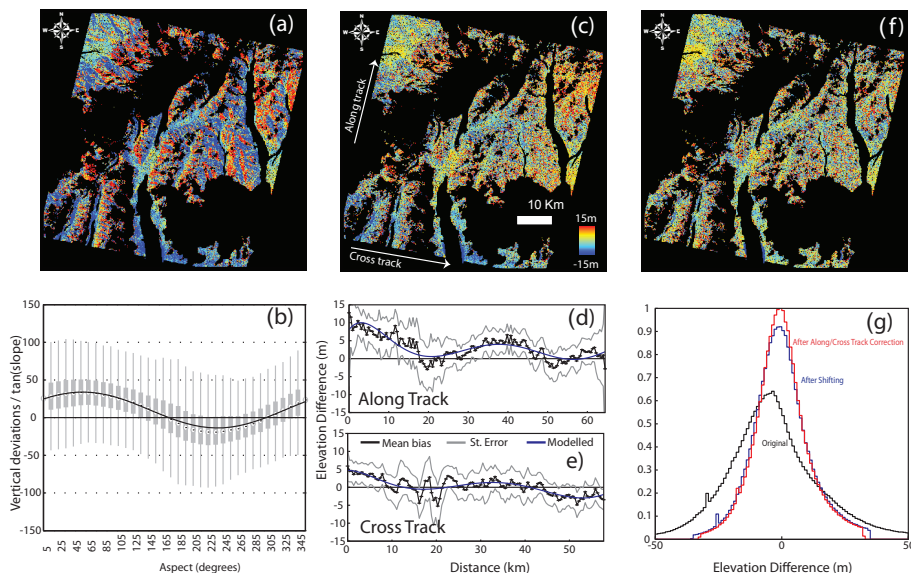


**Fig. 6.** The processing sequence applied to the 2006 ASTER DEM as compared to the SRTM DEM. **(a)** shows the original elevation differences while **(b)** shows the first iteration relationship to aspect and the cosine-fit solution. **(c)** shows the elevation differences after correcting for the shift and **(d)** and **(e)** shows the residual relationship to the along track and cross track directions, respectively, and the polynomial correction. **(f)** shows the elevation differences after the along and cross track corrections. **(g)** shows the final histograms of the three elevation difference maps of (a), (c) and (e). All glaciers, lakes, ocean and outliers due to clouds are masked out in black.

Title Page

Abstract

Introduction

Conclusions

References

Tables

Figures

◀

▶

◀

▶

Back

Close

Full Screen / Esc

Printer-friendly Version

Interactive Discussion



## Correcting elevation data for glacier change detection

C. Nuth and A. Kääb

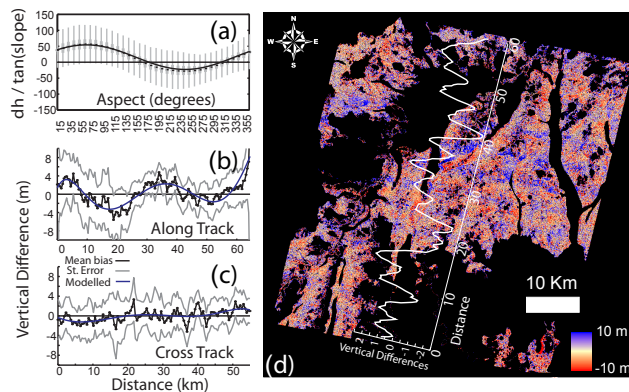


**Fig. 7.** (a), (b) and (c) show the first three corrections applied between two ASTER SilcAst DEMs from 2006 and 2002. (d) shows the resulting elevation differences with a plot of the mean elevation differences along track. The linear cross-track features that run along track seem to have an amplitude of 1–2 m in the vertical direction. These fluctuations are thought to be induced by unrecorded pitch variations of the satellite, *jitter*.

[Title Page](#)
[Abstract](#)
[Introduction](#)
[Conclusions](#)
[References](#)
[Tables](#)
[Figures](#)
[◀](#)
[▶](#)
[◀](#)
[▶](#)
[Back](#)
[Close](#)
[Full Screen / Esc](#)
[Printer-friendly Version](#)
[Interactive Discussion](#)

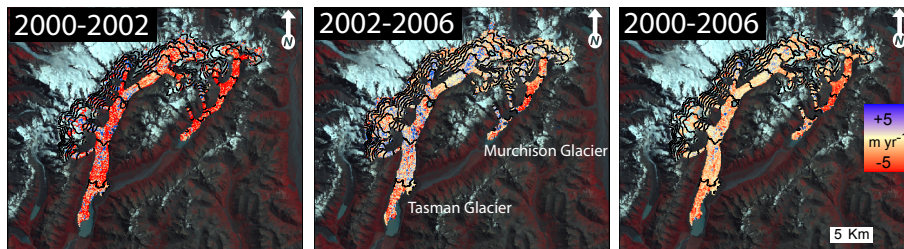


**Fig. 8.** Elevation changes on the Tasman and Murchison Glaciers from 2000–2002, 2002–2006, 2000–2006. The relative small elevation changes of these glaciers means that the bias induced from both the ASTER scenes and the SRTM will have a large impact on estimates. We therefore do not show elevation change relationships with elevation because it became clear that the high frequency sinusoidal pattern of Fig. 7d is superimposed within the change measurements.

**Correcting elevation data for glacier change detection**

C. Nuth and A. Kääb

Title Page	
Abstract	Introduction
Conclusions	References
Tables	Figures
◀	▶
◀	▶
Back	Close
Full Screen / Esc	
Printer-friendly Version	
Interactive Discussion	



Correcting elevation data for glacier change detection

C. Nuth and A. Kääb

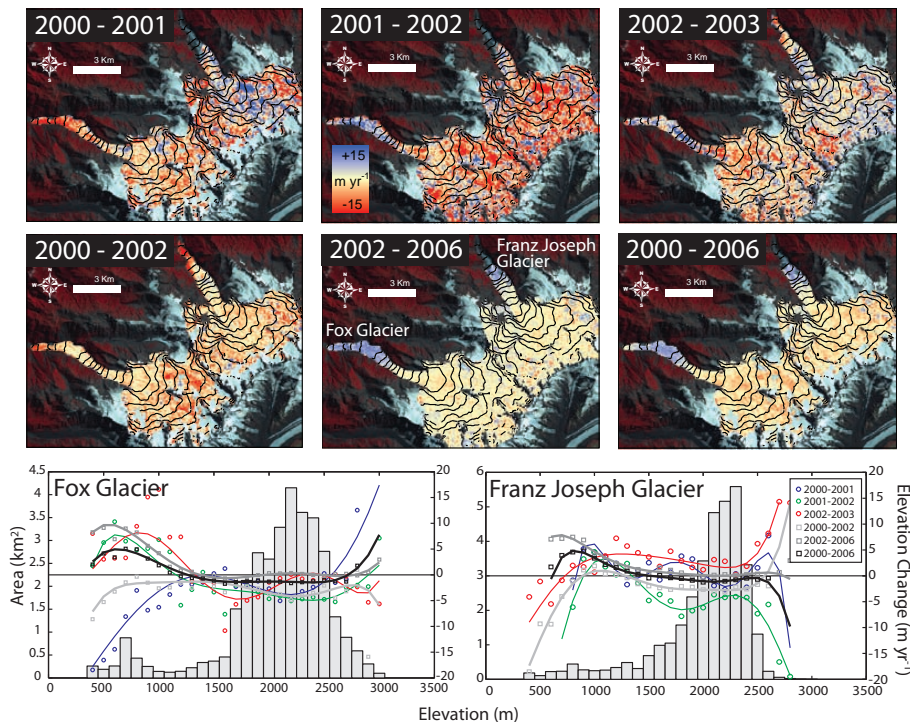


**Fig. 9.** Elevation changes on the Fox and Franz Joseph Glaciers. The top three images show elevation differences calculated in single years while the middle 3 images are multi-year elevation differences. Clearly apparent is the reduction of noise in the multi-year differences as opposed to the single year differences. Elevation change averages per elevation and associated glacier hypsometry of both glaciers is shown in the lower figures for all the above named differences.

Discussion Paper | Discussion Paper | Discussion Paper | Discussion Paper

Title Page

Abstract

Introduction

Conclusions

References

Tables

Figures

◀

▶

◀

▶

Back

Close

Full Screen / Esc

Printer-friendly Version

Interactive Discussion



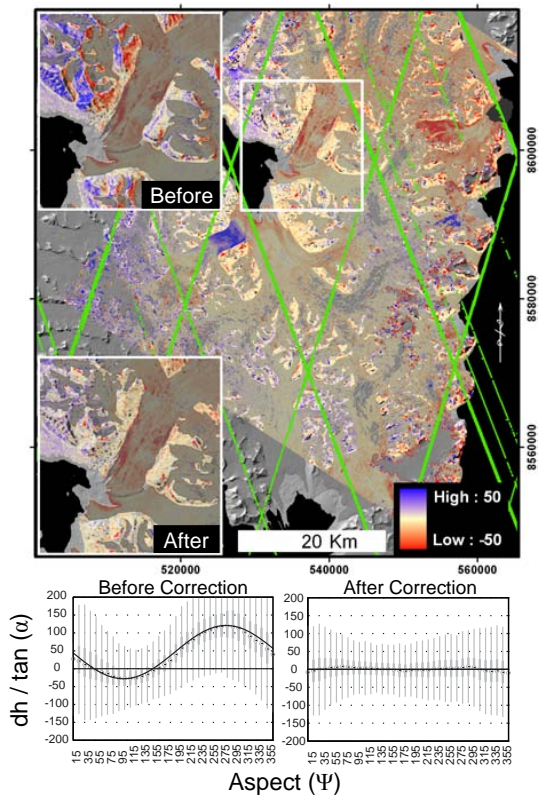


**Fig. 10.** Top: Elevation differences before and after shifting the ASTER DEM to the SPOT5-HRS DEM. The final shift is  $\approx 2.5$  ASTER pixels to the west-north-west. The green lines are the ICESat tracks. Bottom: The sinusoidal relationship with aspect before the shift, and the lack of one after shifting.

**Correcting elevation data for glacier change detection**

C. Nuth and A. Kääb

Title Page

Abstract Introduction

Conclusions References

Tables Figures

◀ ▶

◀ ▶

Back Close

Full Screen / Esc

Printer-friendly Version

Interactive Discussion



## Correcting elevation data for glacier change detection

C. Nuth and A. Kääb

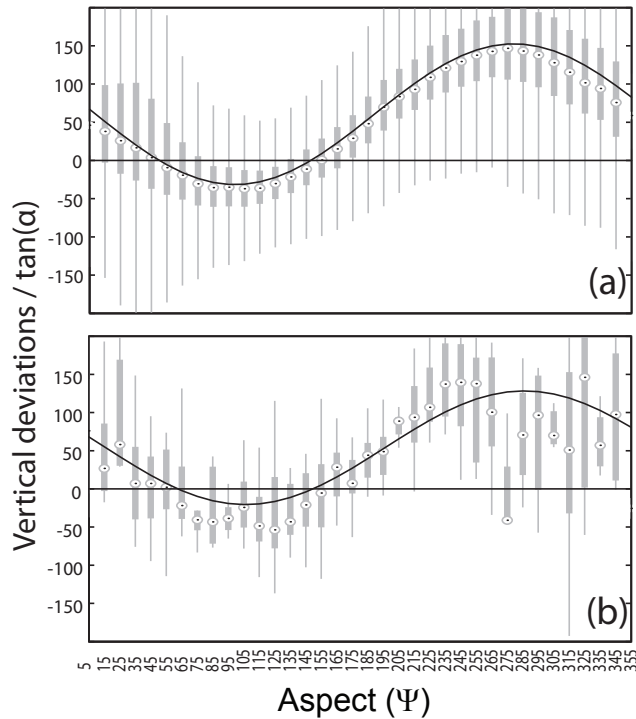


**Fig. 11.** The first iteration of the co-registration between the ASTER DEM and the aerophotogrammetric DEM **(a)** and the ASTER DEM and ICESat **(b)**.

Title Page

Abstract

Introduction

Conclusions

References

Tables

Figures

◀

▶

◀

▶

Back

Close

Full Screen / Esc

Printer-friendly Version

Interactive Discussion



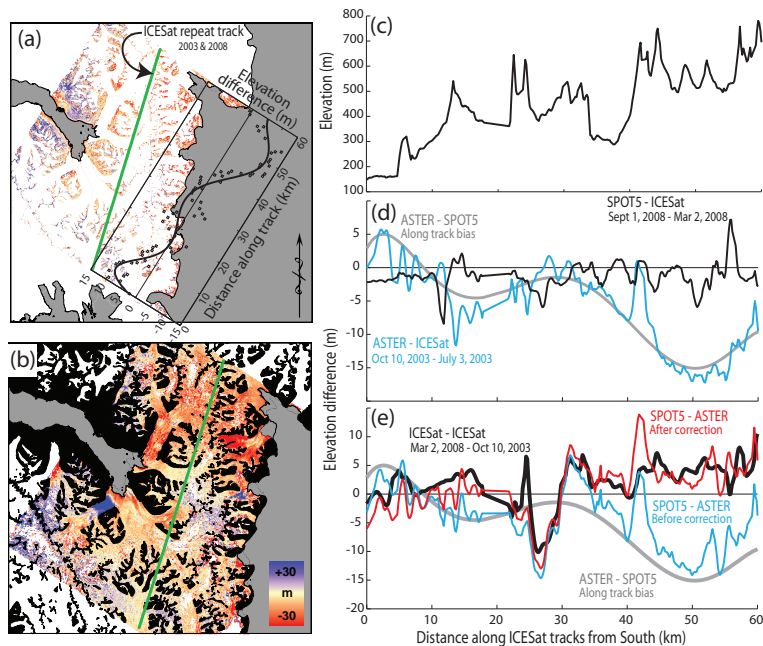


**Fig. 12.** Elevation differences between the SPOT5-HRS and ASTER DEMs over the non-glaciated regions (a) and the glaciated regions (b). The graph inset in (a) shows the along track bias measured from the stable terrain and the 6th order polynomial correction. The green line is an ICESat repeat track from 10 October 2003 and 2 March 2008. The elevation profile from the 2003 ICESat track is shown in (c), The differences between DEMs and the ICESat track closest in time to the DEM acquisition is compared (d). The difference of the ASTER DEM is similar to the bias correction as determined between the two DEMs. The elevation changes between 2008 and 2003 are shown in (e) before and after correcting for the along track ASTER bias. ICESat to ICESat differences are made by a simple along track interpolation as the cross track separation was not greater than 15 m, which is well within the footprint size of ICESat.

## Correcting elevation data for glacier change detection

C. Nuth and A. Kääb

Title Page

Abstract

Introduction

Conclusions

References

Tables

Figures



Back

Close

Full Screen / Esc

Printer-friendly Version

Interactive Discussion



## Correcting elevation data for glacier change detection

C. Nuth and A. Kääb

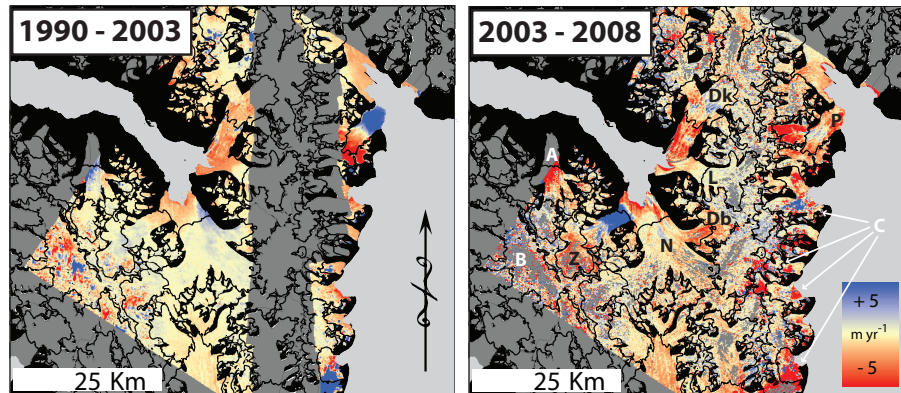


**Fig. 13.** Elevation changes from 1990–2003 and 2003–2008 after co-registration and adjusting for along/cross track biases. In the 2003–2008 image, we denote data artifacts using white upper case letters in which [A] and [B] are edge effects and [C] are cloud anomalies. Black upper case letters represent individual glacier trends described in the text; [Z] Zawadskibreen, [N] Nathorstbreen, [Db] Dobrowolskibreen, [L] Liestølbreen, [Dk] Doktorbreen, [P] Perseibreen.

Title Page

Abstract

Introduction

Conclusions

References

Tables

Figures

◀

▶

◀

▶

Back

Close

Full Screen / Esc

Printer-friendly Version

Interactive Discussion



## Correcting elevation data for glacier change detection

C. Nuth and A. Kääb

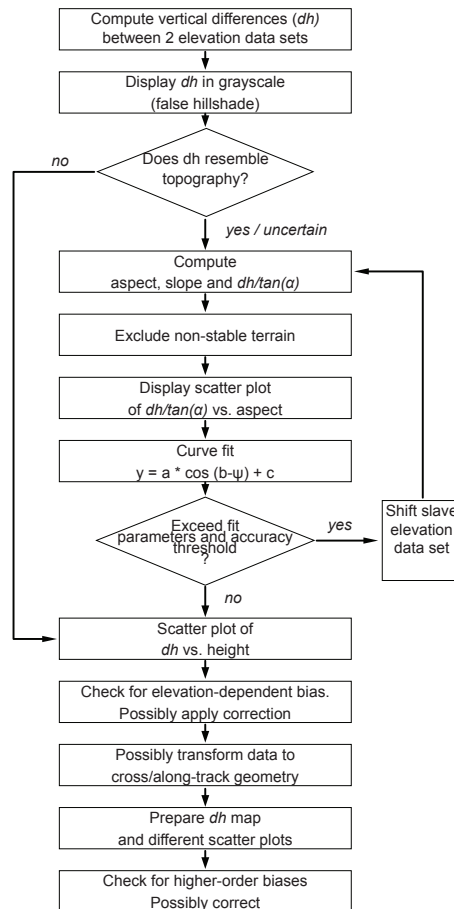


**Fig. 14.** A suggested methodology for comparing DEMs or elevation products for glacier change detection.

[Title Page](#)
[Abstract](#)
[Introduction](#)
[Conclusions](#)
[References](#)
[Tables](#)
[Figures](#)
[◀](#)
[▶](#)
[◀](#)
[▶](#)
[Back](#)
[Close](#)
[Full Screen / Esc](#)
[Printer-friendly Version](#)
[Interactive Discussion](#)
